symmetry

MDPI

Review

Chiral Buckybowl Molecules

Kuppusamy Kanagaraj [1,†], Kangjie Lin [1,†], Wanhua Wu [1], Guowei Gao [1], Zhihui Zhong [2], Dan Su [2] and Cheng Yang [1,*]

[1] Key Laboratory of Green Chemistry & Technology, College of Chemistry, Sichuan University, Chengdu 610064, China; kanagaraj195@gmail.com (K.K.); kangjie_lin@outlook.com (K.L.); wuwanhua.510@163.com (W.W.); gaoguowei@scu.edu.cn (G.G.)

[2] State Key Laboratory of Biotherapy, West China Medical Center, Sichuan University, Chengdu 610064, China; zhihui.zhong@hcbiomed.com (Z.Z.); sudan.lab@hotmail.com (D.S.)

* Correspondence: yangchengyc@scu.edu.cn; Tel.: +86-28-8541-6298

† These authors contributed equally to this paper.

Received: 27 July 2017; Accepted: 21 August 2017; Published: 30 August 2017

Abstract: Buckybowls are polynuclear aromatic hydrocarbons that have a curved aromatic surface and are considered fragments of buckminsterfullerenes. The curved aromatic surface led to the loss of planar symmetry of the normal aromatic plane and may cause unique inherent chirality, so-called bowl chirality, which it is possible to thermally racemize through a bowl-to-bowl inversion process. In this short review, we summarize the studies concerning the special field of bowl chirality, focusing on recent practical aspects of attaining diastereo/enantioenriched chiral buckybowls through asymmetric synthesis, chiral optical resolution, selective chiral metal complexation, and chiral assembly formation.

Keywords: buckybowl; corannulene; sumanene; bowl chirality; bowl inversion; asymmetric synthesis; chiral resolution

1. Introduction

Studies on the physical and chemical characteristics of buckybowls have attracted significant interest owing to their direct structural correlation with fullerenes and potential applications in the realm of material science (Figure 1) [1–3]. Corannulene **1** and sumanene **2**, two prototypical buckybowls, are both highly curved π-conjugated aromatic molecules representing the substructures of fullerene. The smallest C_{3v}-symmetric fragment **2** comprises a central six-membered ring surrounded by three five- and three six-membered rings fused in an alternating fashion (Figure 1), whereas the smallest C_5-symmetric fragment **1** contains a central five-membered ring surrounded by five six-membered rings (Figure 1). Regioselective allocation of the five- or six-membered ring subunits around the centroid pentagon or hexagon, respectively, gave the curved bowl-shaped structures. Certain buckybowls are inherently chiral and difficult to separate from the racemates due to their rapid bowl inversion [4]. Controlling the bowl chirality of these π-conjugates and obtaining enantioenriched buckybowls are challenging tasks for chemists, while buckybowls application in chiral materials is highly promising [5–14]. Further extension of the π-conjugation of these chiral enantioenriched buckybowls leads to homochiral carbon nanotubes, and these chiral carbon materials create new perspectives in chiral catalysis, chiral sensing, chiral separation sciences, etc. [15–27]. A better understanding of bowl chirality will help researchers find a good way to control the chiral self-assembly of carbon nanotubes (CNTs) or fullerenes, which have already exhibited exciting potential as next-generation functional materials [28–38].

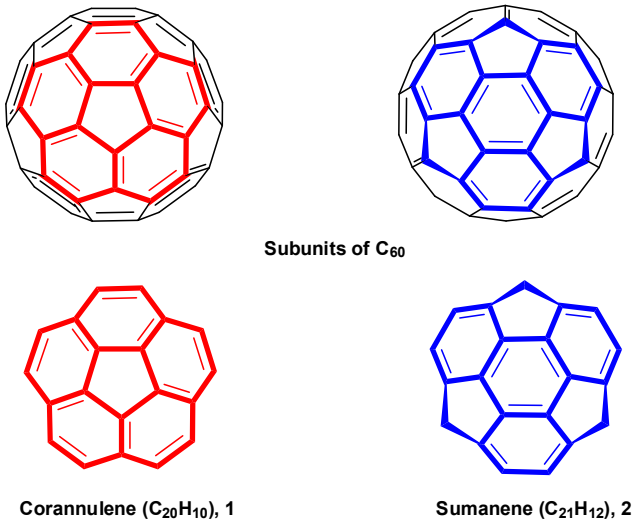

Figure 1. Chemical structures and bowl-shaped fragments of **1** (**left**) and **2** (**right**) as rim hydrogenated subunits of spherical buckminsterfullerene C_{60}.

While several buckybowl-related reviews have been published in recent years [6,39–44], most of them focused on the synthetic strategy and derivation method. Only a few publications involve the stereochemistry or chirality of the buckybowls. In this short review, we summarize recent progress on the stereochemistry of buckybowls and their derivatives. It covers recent developments in the asymmetric synthesis and optical resolution of buckybowls from their racemates, and application of the enantioenriched buckybowls in the chiral aggregate formation and homochiral CNT syntheses [45,46]. These structurally well-defined single-chiral CNTs exploit truly exciting applications ranging from space elevator to armchair quantum wire and bio-related applications [47]. Chiral buckybowls that possess a stable concave or convex shape are suitable for the construction of chiral molecular recognition sites [48]. They may also coordinate metals by virtue of their electron-rich/-deficient properties and thus have the potential for enantioselective organocatalysis [49,50]. Chiral buckybowls, acting as chiral building blocks, can also be used for constructing helical assemblies and preparing homochiral crystalline organic materials.

2. Classification of Bowl Chirality

Bowl-shaped carbon-based π-conjugated aromatic compounds, so-called "buckybowls", are the partial structure of fullerenes or CNTs (Figure 1). These three-dimensional (3D) curved π-electron systems may possess inherent chirality and present many similarities to chiral fullerenes and CNTs, which is often defined as "bowl chirality" for convenience. The bowl-shaped polyaromatic hydrocarbon chiral buckybowl molecules can be broadly classified into three categories (Figure 2) based on the origin of their chirality. The conjugated bowl structure itself possesses the chirality, such as π-extended buckybowls, e.g., hemifullerene **3**; bowl chirality caused by introduction of one or more substituents on the rim of the buckybowl, e.g., trimethylsumanene **4**; and bowl chirality originated from the introduction of heteroatom into the π-bowl carbon skeleton, e.g., triazasumanene **5**.

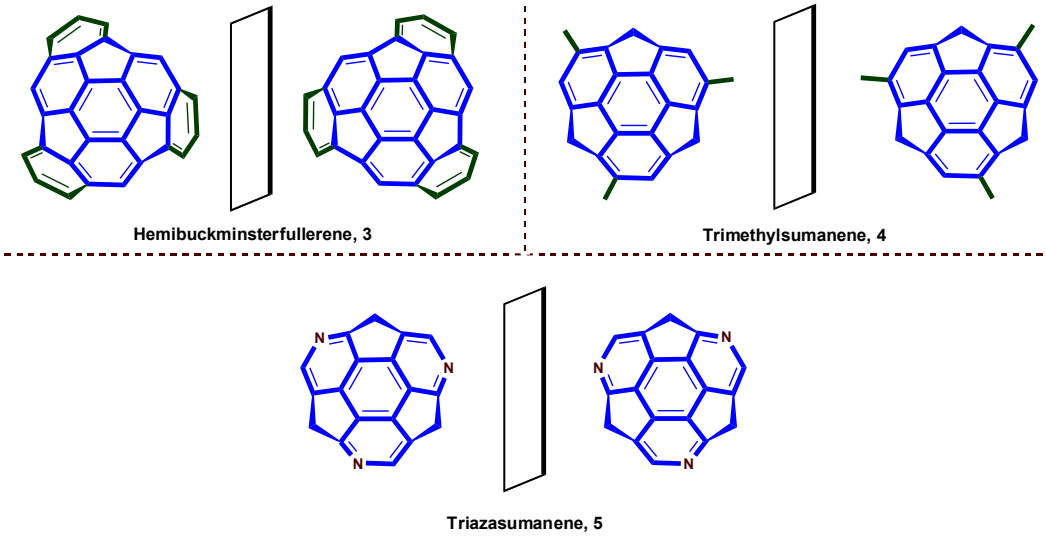

Figure 2. Classification of chiral buckybowl molecules.

Unlike common aromatic compounds, which often have a symmetry plane along the aromatic ring, buckybowls loss the cross-ring symmetry plane due to the curved shape. Unsubstituted buckybowls **1** and **2** are not chiral due to the presence of the reflection symmetry with respect to the mirror planes containing the rotational axis to show C_{5v} and C_{3v} symmetry, respectively. Introducing the addends may break the reflection symmetry to cause chirality, and alter their properties, such as bowl-to-bowl inversion [12–22], chirality [12,17,19,23], bowl depth [14,19,20], crystal structure [19,24,25], molecular recognition [2,26,27,51] and supramolecular assembly [3,28–30,52,53] behavior, metal complexation [23,31–36], electronic conductivity [19,37,38], and so on. Although the chirality is an important element in three-dimensional curved π-electron systems, thus far there have been no reports of the enantioselective synthetic control of the bowl chirality.

3. Stereodescriptor System of Buckybowls

Until now, the absolute configuration of bowl chirality of chiral buckybowl molecules was followed by two independent stereodescriptor systems: The stereodescriptor *C* or *A* based on fullerene nomenclature [17,54] and the another stereodescriptor *P* or *M* based on the Cahn–Ingold–Prelog (CIP) sequence rule [32]. The numbering system of fullerenes follows in general a helical numbering path, starting from the lowest set of numbers for substituents. To assign a descriptor in the chiral fullerene system, the viewer looks from the outside of the fullerene cage at the polygon to start the numbering and trace the path of numbering C(1)–C(6) (Figure 3a) [54]. The chirality of buckybowls is assigned in the same way, and a viewer looks from the convex face and traces the path of numbering from atom C(1) to C(6) (Figure 3b) [17]. If the numbering path describes a clockwise direction/travel, the configuration of the chiral bowl is designated as *C*. In contrast, if the path describes a counterclockwise direction/travel, the configuration of the chiral bowl is designated as *A*.

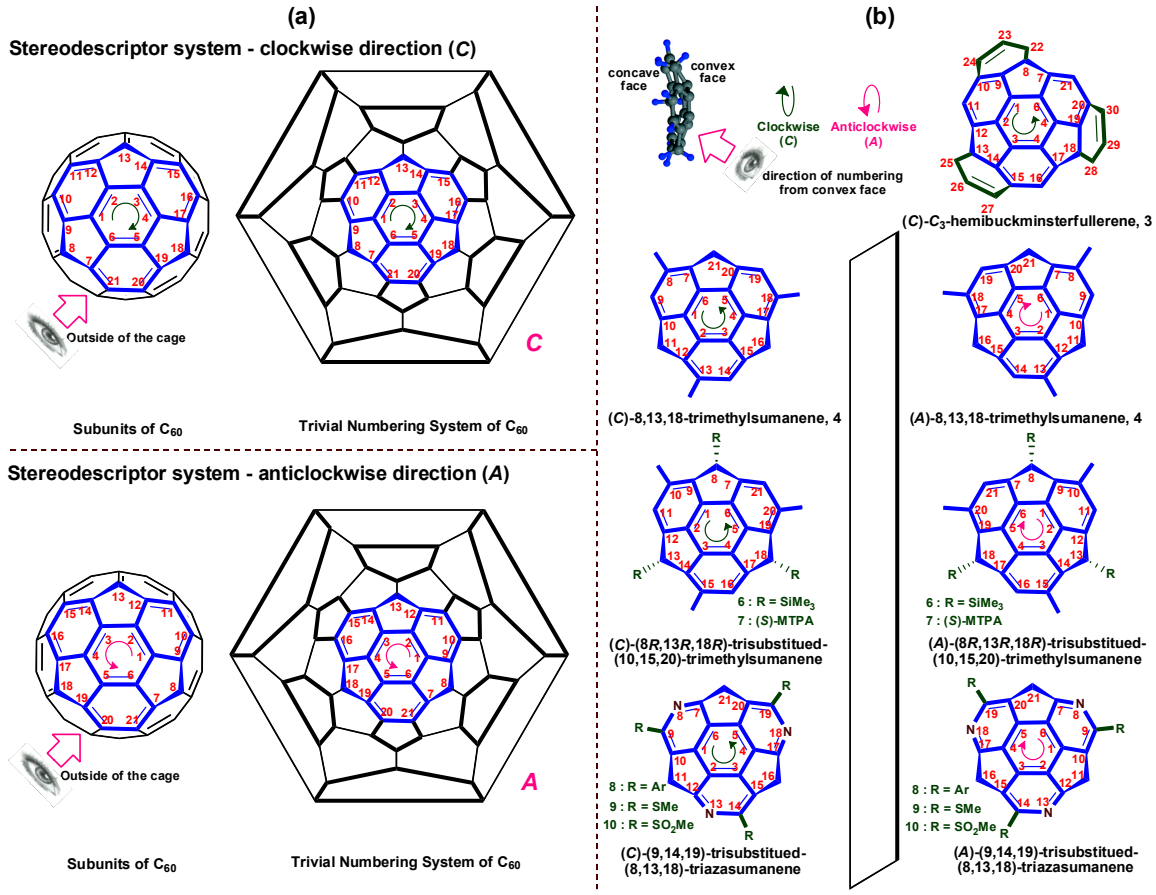

Figure 3. (**a**) Three-dimensional diagram of C_{60} with the subunit of sumanene including enantiomeric travel numbering schemes and the related stereodescriptor systems *C* and *A*; (**b**) The stereodescriptor system of some C_3 symmetric chiral buckybowls.

Another stereodescriptor system *P* or *M* for chiral buckybowls uses the CIP sequence rule [32]. Based on the CIP priority rule [55], the "non-fusion peripheral atoms" of buckybowl molecules are compared, and one atom with the highest CIP priority is chosen as the first priority (point of origin, ①, Figure 4) [17,18]. Furthermore, for the next highest CIP priority atom ② versus ①, compare the two neighboring rim atoms attached to this original point, and subsequent atoms attached thereto. For a viewer looking from the concave face of the buckybowl molecule, i.e., looking "into" the cavity of the bowl, the path of CIP priority numbering is from the original point atom to the neighboring atom with higher priority (①→②). If the path of CIP priority numbering direction describes clockwise travel, the configuration of the chiral bowl is designated as *P*. Otherwise, if the path of CIP priority numbering travels in a counterclockwise direction, the descriptor is *M*. The numbering to specify the positions of substituents follows the nomenclature of fused ring systems.

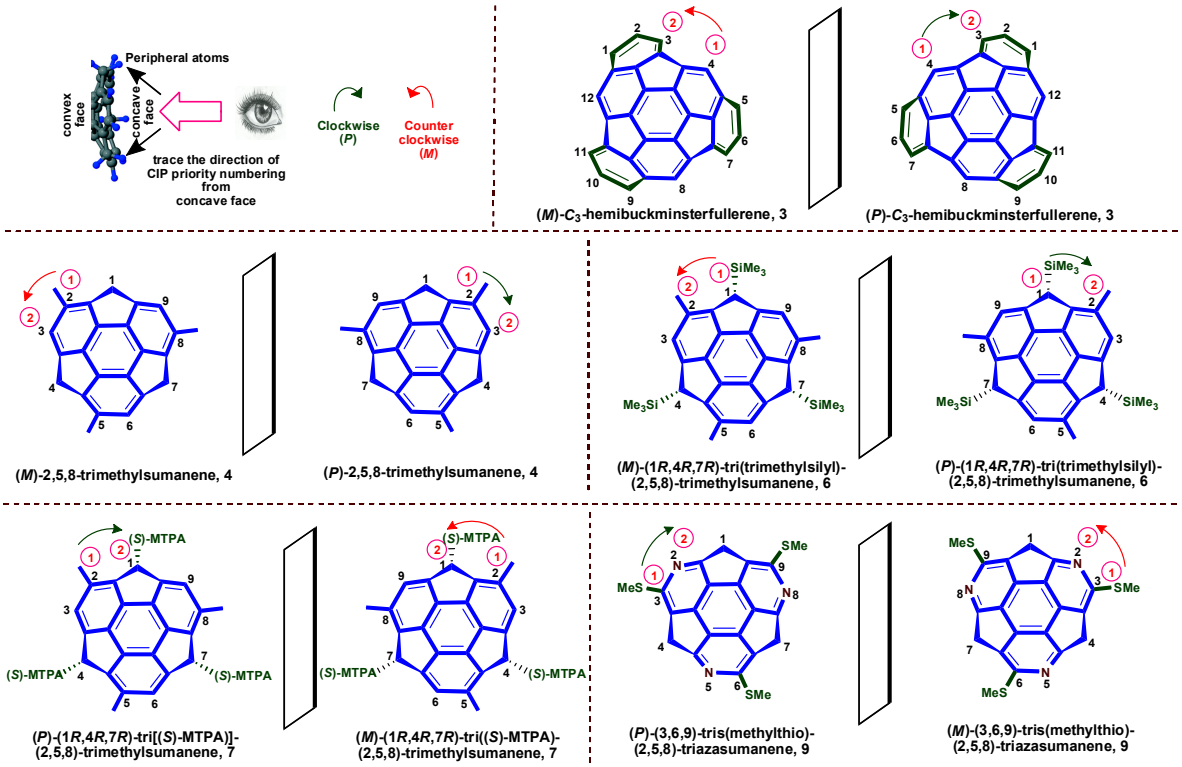

Figure 4. The *P* and *M* stereodescriptor system for some C_3 symmetric chiral buckybowl molecules based on the CIP priority rule.

4. Bowl Inversion/Racemization of Chiral Buckybowls

A unique property of buckybowls lies in that these molecules can thermally flip their curvature in solution via bowl-to-bowl inversion or concave–convex transition. During the bowl inversion process, the inherent bowl chirality inverts; this process is also called racemization (Figure 5a) [12,17–19]. The nonpolar polyaromatic small bowl molecules, like **1** and **2** can thermally flip through a planar transition state and the required energy to cross this transition barrier is defined as bowl inversion energy (ΔE) (Figure 5b) [20]. In the solid state, buckybowl molecules exist in a stack structure and show excellent physical properties, such as electron conductivity [24].

The thermally driven bowl-to-bowl inversion is of interest to basic science and can find various applications in functional materials for sensors, chemical machines, or ferroelectric memories. The lifetime of enantiopure chiral buckybowls is controlled by the bowl inversion energy (ΔE). The enantiopure chiral buckybowls are expected to contribute to a variety of applications such as asymmetric molecular recognition, homochiral crystal organic materials, chiral self-assembly, and chiral organometallic catalysis [6,7,9].

The introduction of substituents or heteroatoms in the carbon skeleton of buckybowls changes the bowl inversion energy within the range of 20–40 kcal/mol, and therefore could change the lifetimes of chiral buckybowls considerably. Furthermore, the nature, position, number of substituents, and stereoelectronic effects also significantly influence the bowl shape, depth (x), lifetime of keeping chirality, electron-deficient/-rich nature, and other physicochemical properties [56]. The bowl-inversion energy of corannulene derivatives was first determined by Scott and co-workers [13]. The interesting dynamic behavior of various buckybowl molecules has been extensively studied by Scott [57], Siegel [14,16], Hirao [15,35], Sakurai [12,17–20], and others. In particular, Sakurai and co-workers studied the effect of the substituent R at the benzylic position of sumanene **11**, which possesses two different conformers, *endo*-R and *exo*-R, differing in the direction of the aromatic bowl shape, concave or convex (Figures 6 and 7) [56].

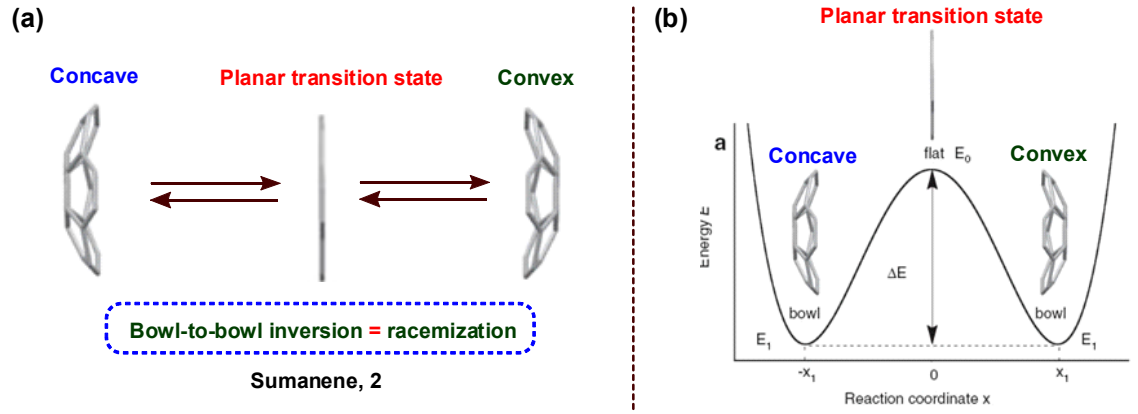

Figure 5. (**a**) Racemization of chiral **2** through bowl-to-bowl inversion/racemization; (**b**) the double-well potential energy profile. Reprinted from [20]. © 2014 Pure & Applied Chemistry.

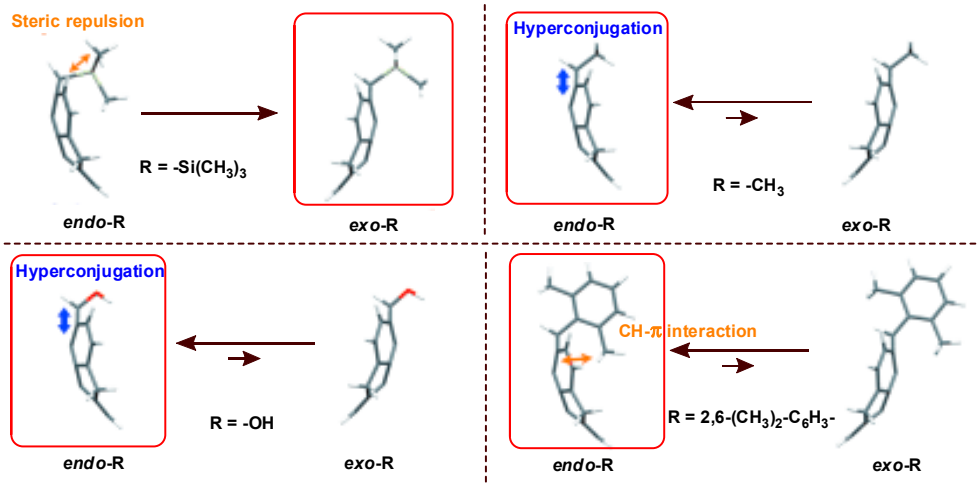

Figure 6. The *endo*-R and *exo*-R conformers of monosubstituted-sumanene **11** as determined by DFT calculations and the involved stereoelectronic effects. Reprinted from [56]. © 2013 Wiley-VCH Verlag GmbH & Co. KGaA, Weinheim.

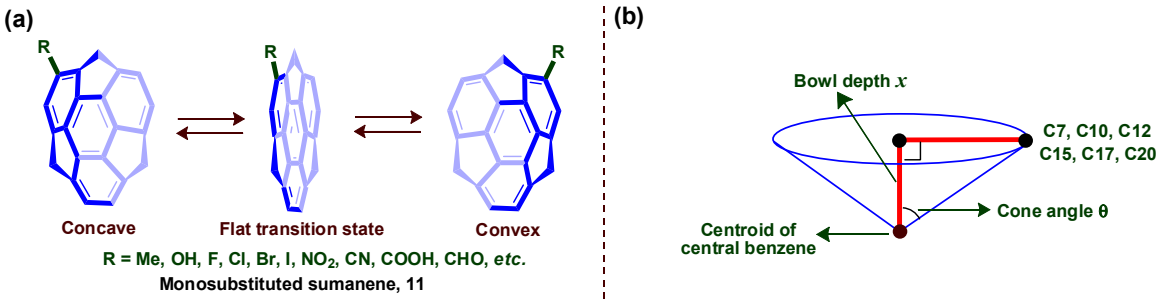

Figure 7. (**a**) Monosubstituted sumanene derivatives **11**; (**b**) Its graphical representation bowl depth and cone angle.

Introduction of substituents will influence the geometries/conformations of buckybowls and bowl inversion energies as well. The effect of substituents in corannulene has been studied by Siegel and co-workers [14,16]. They demonstrated that introducing the acyclic substituents in corannulene usually decreases the bowl depth and increases the bowl inversion energy. Based on the results of the experimental and theoretical study, they proposed a quantitative equation for bowl inversion energy,

which relates the bowl depth to the bowl inversion energy (Figure 7) [14,16]. Steric and electronic factors of substituents also affect the bowl structure and bowl inversion energy of sumanene. Recently, Sakurai and co-workers found that sumanene **2** attached with a mono-iodo substituent induces a slightly deeper bowl depth and a higher bowl inversion energy compared with other sumanene derivatives because of its steric effect, whereas the electronic effects caused by formyl and nitro substituents induced a shallower bowl depth and a lower bowl inversion energy [20].

Siegel and co-workers studied the bowl-to-bowl inversion of corannulene **1** and ethylcorannulene derivatives mediated by extended tetracationic cyclophane (Figure 8) [22,30]. This synthetic host forms a supramolecular complex with **1** and ethylcorannulene via induced fit, and the bowl-to-bowl inversion process was accelerated by a factor of 10 at room temperature. Upon host–guest complexation, the transition state of the guest is stabilized through the stereoelectronic reorganization of the host, which switched from a strained conformation to an energetically favored conformation. Further, the experimental and DFT calculations for bowl-to-bowl inversion process of the host-guest complexion of **1** demonstrates the decrease of bowl-to-bowl inversion energy barrier of corannulene (Figure 8).

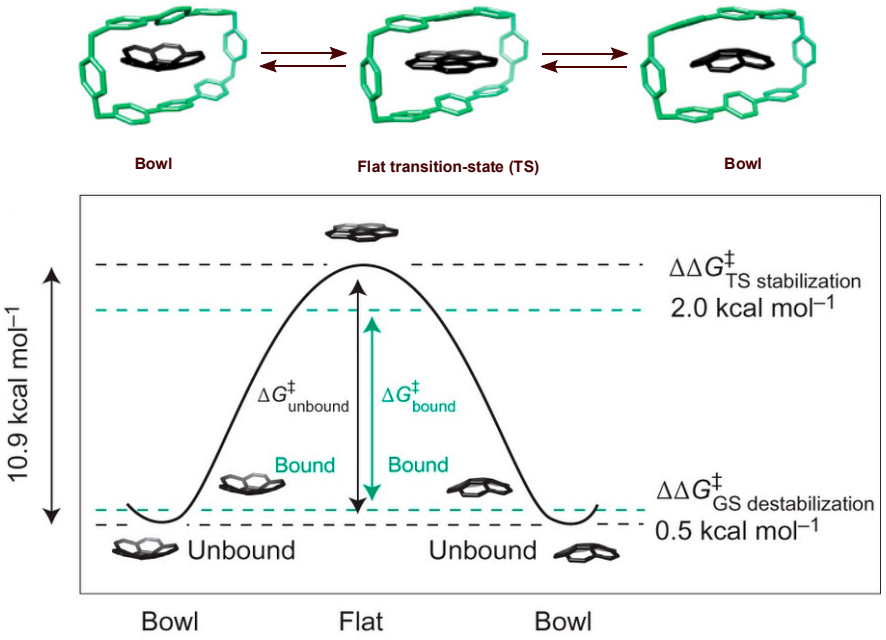

Figure 8. Comparison of energy profile of bowl-to-bowl inversion of corannulene **1** (black) and tetracationic cyclophane: **1**, complex (green) in Me_2CO; absolute contributions of ground-state (GS) destabilization (0.5 kcal mol^{-1}) and transition-state (TS) stabilization (2.0 kcal mol^{-1}) to the overall energy-barrier decrease ($\Delta\Delta G^{\ddagger}_{catalysis}$) of the bowl-to-bowl inversion process of **1** inside the tetracationic cyclophane calculated by DFT (B97D/Def2-TZVPP). Reprinted from [22]. © 2014 Nature Publishing Group.

5. Heterobuckybowls

Doping of heteroatoms to the carbon frameworks of bowl-shaped aromatic compounds drastically modulates their geometrical structure and physical and chemical properties. After the successful synthesis of corannulene and sumanene derivatives, researchers began to try to synthesize hetero atom-doped buckybowl molecules, so-called "heterobuckybowls". The introduction of heteroatoms into the carbon skeleton is expected to yield altered electronic properties of basic carbon skeleton buckybowls, especially electron-deficient or -rich in nature. Notably, the substitution of a hetero atom in its carbon skeleton also causes the geometrical change, especially the depth of the bowl. As a result of the change in depth of the bowl, the activation energy for the bowl-to-bowl inversion energy is also altered. The higher the bowl inversion energy is, the more stable the chiral conformer will be. Several heterobuckybowls have been reported in the literature, some of them chiral (Figure 9) [12,58–66].

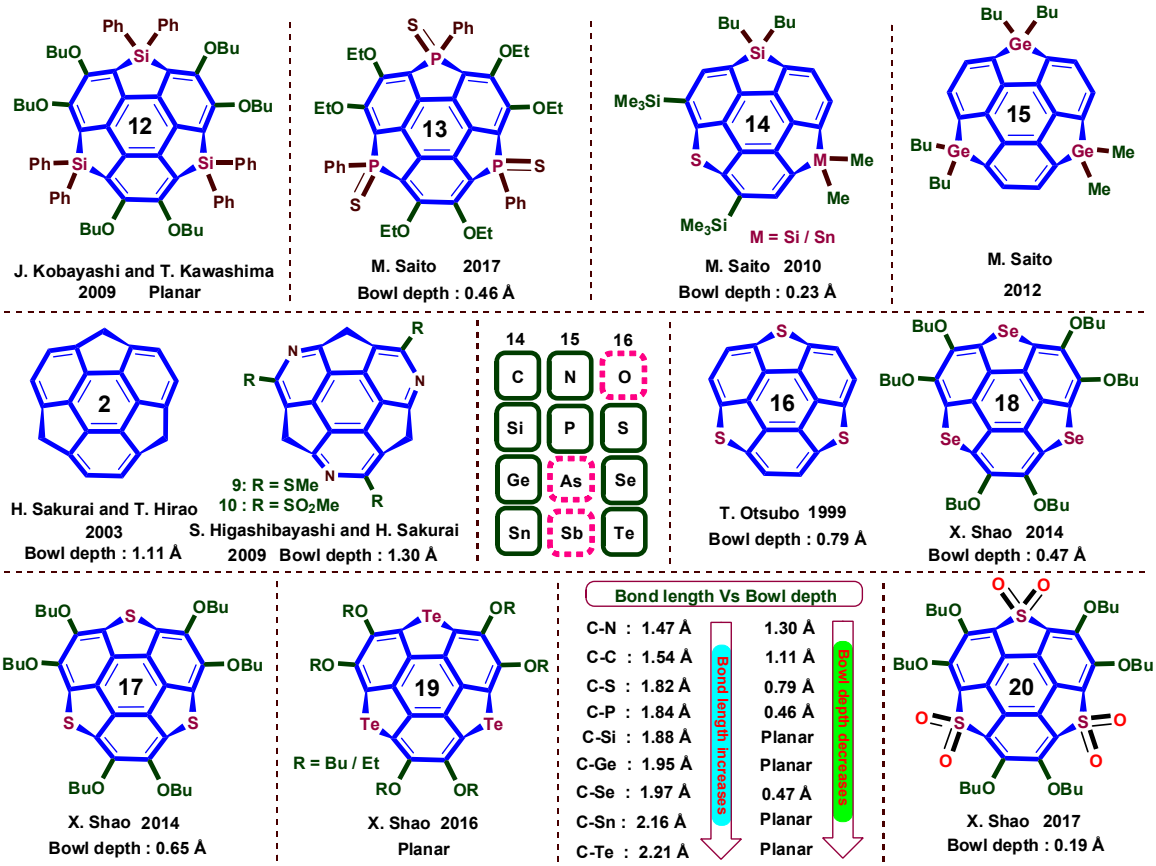

Figure 9. Heterobuckybowls with their bowl depth.

The heteroatoms embedded in the reported heterobuckybowls are mainly the group 14, 15, and 16 elements, such as nitrogen (second row), silicon, phosphorus and sulfur (third row), germanium and selenium (fourth row), and tin and tellurium (fifth row) (Figure 9). Introduction of heteroatoms in the periphery of buckybowls usually resulted in a decrease of the bowl depth of heterobuckybowls, because the bond lengths of carbon–heteroatom increased with the atomic size (Figure 9). The bowl depths of trithiasumane **16** (0.79 Å) and triselenasumane **18** (0.47 Å) [64] have a shallower bowl depth than that of normal sumanene **2** (1.11 Å) [24]. Trisilicasumanene **12** [59,63] and tritellurasumanene **19** have a plane structure, whereas triazasumanene **10** has a deeper bowl depth of 1.30 Å because the C–N bond length (1.47 Å) is shorter than the C–C bond length (1.54 Å) [12]. The high reactivity of nitrogen facilitates the formation of the highly strained triazasumanene derivative with higher bowl-to-bowl inversion energy. More recently, Saito and co-workers prepared a triphosphasumanene trisulfide **13** derivative with a large dipole moment (12.0 D) [67]. The bowl depth of *syn*-isomer **13** is 0.46 Å, which is identical to triselenasumane **18** (0.47 Å) [64] and shallower than sumanene [24], whereas the *anti*-isomer of triphosphasumanene trisulfide **13** exists in an almost plane structure [67].

6. Asymmetric Synthesis of Buckybowl and Azabuckybowl

Synthesis of buckybowls was a highly challenging task for chemists. The first synthesis of the pristine corannulene was accomplished in 1966 by applying a long synthetic route [68]. The synthetic investigation was postponed until Scott et al. [69] and Siegel et al. [70] reinitiated the synthesis of corannulene with a succinct synthetic route by using the flash vacuum pyrolysis (FVP) method in the early 1990s. In the FVP method, the planar π-conjugated precursors are directly converted into buckybowls under high temperature to yield a racemic mixture [71]. Many buckybowls were thus synthesized using this FVP method, whereas FVP method was unsuccessful for the synthesis of **2** [72]. In 1996, Siegel and co-workers

developed the first solution phase synthesis of **1** [73]. Adopting this simple and short solution phase strategy, another pristine buckybowl **2** was obtained by Sakurai and co-workers [74].

In 2008, Sakurai and co-workers reported the first asymmetric synthesis of trimethylsumanene **4** using stepwise conversion strategy under milder reaction conditions [17]. The synthetic strategy is described in Scheme 1.

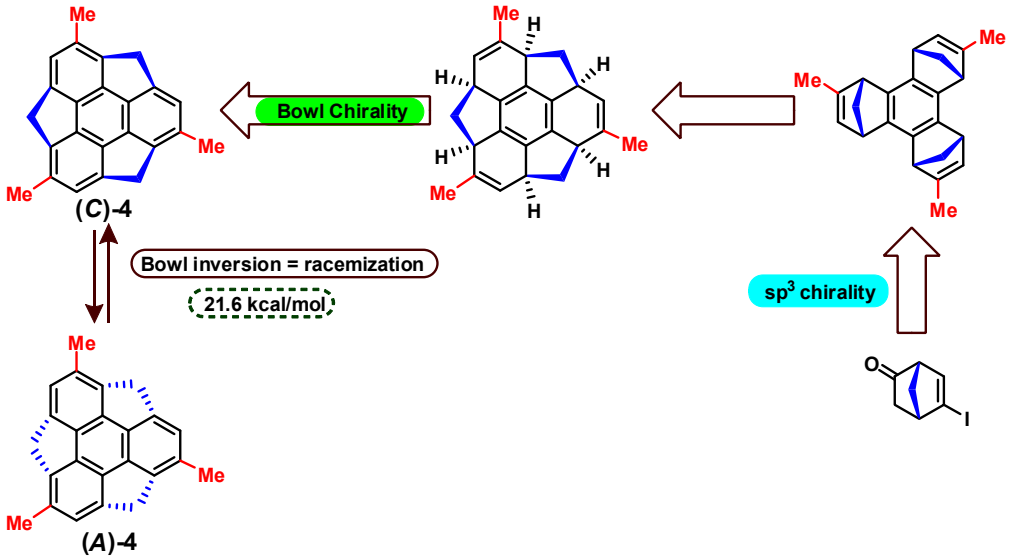

Scheme 1. Strategy for the asymmetric synthesis of chiral (*C*)-trimethylsumanene **4**.

In this strategy, chiral norbornene possessing stereogenic carbon center was used as the precursor, which was converted into planar nonconjugated bowl by Pd catalyzed *syn*-selective cyclotrimerization [75,76], and the sp^3 chirality was thus transmitted to the bowl chirality of **4**. The key concern of this strategy is the rate of racemization, which is directly correlated to the inversion barrier of buckybowls. Many buckybowls have a low bowl-to-bowl inversion barrier at room temperature and are unable to separate their enantiomers. For example, most corannulene derivatives are not able to enantiomerically isolate because of their bowl inversion energy of ca. 11.5 kcal/mol (bowl-bowl-inversion is >20,000 times per second at room temperature) [14]. In contrast, the bowl inversion energy of **2** and **4** is around 20.3 kcal/mol (one time per 143 s) [15,19] and 21.6 kcal/mol [19], respectively. Since the half-life of the bowl inversion of **4** are 2 h at 0 °C and 23 min at 20 °C [17], the isolation of an enantiomer would be possible if the last aromatization step is carried out at a low temperature.

Thus, the aromatization step, converting the nonconjugated bowl into a conjugated bowl, was carried out using excess DDQ in a very short reaction time (1 min) at 0 °C, and the resulting (*C*)-**4** quickly purified at <−20 °C. The isolated (*C*)-**4** was stored at −80 °C. The chirality of (*C*)-**4** was analyzed by the circular dichroism (CD) spectra at −40 °C, which show two positive Cotton effect curves at 247 nm and 284 nm, respectively (Figure 10a). In contrast, the intensity of CD signals gradually decreased at 10 °C (Figure 10b), indicating the racemization of (*C*)-**4** through bowl inversion. The experimentally observed bowl inversion energy is 21.6 kcal/mol, which is close to the calculated value (21 kcal/mol). The chiral (*C*)-**4** was converted into (*C*)-**7** (Scheme 2) using (*S*)-MTPA as a derivatization reagent [17]. The bowl inversion energy barrier of (*C*)-**7** is further increased and the *de* values can be determined using NMR or HPLC analysis.

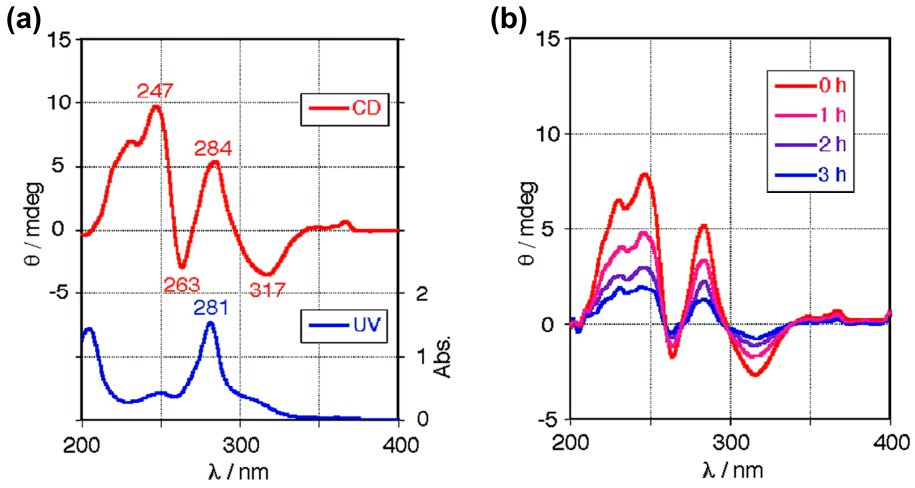

Figure 10. (**a**) CD spectra of (*C*)-**4** in CH_3CN at −40 °C (red line) and UV spectra of (*C*)-**4** in CH_3CN at room temperature (blue line); (**b**) Decay of CD spectra of (*C*)-**4** in CH_3CN at 10 °C for 3 h. Reprinted from [17]. © 2008 American Chemical Society.

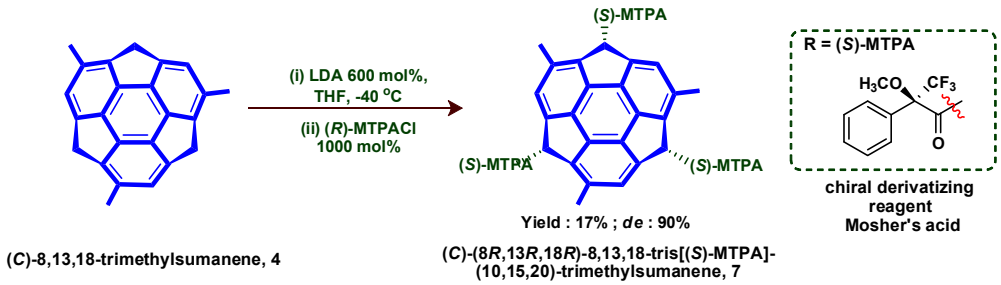

Scheme 2. Derivatization of (*C*)-**4** using chiral derivatizing reagent for the determination of *ee*.

It has been proven that the bowl inversion energy of buckybowls increased with bowl depth [14]. Theoretical studies suggested that doping of nitrogen will lead to deeper and curved bowl depth compared to the all-carbon counterparts [77]. Sakurai and co-workers reported the first chiral nitrogen-doped buckybowl (Scheme 3) [12]. Pure chiral (*C*)-(−)- and (*A*)-(+)-tris(methylthio)triazasumanene **9** was synthesized from corresponding enantiopure nonconjugated simple precursors, which was further converted into corresponding chiral sulfone derivative **10** by oxidation using *meta*-chloroperoxybenzoic acid (*m*-CPBA). From the single crystal analysis, the bowl depth of compound **10** is 1.30 Å, which is deeper than that of **2** (1.11 Å), indicating a higher bowl inversion barrier than the pristine **2**. The bowl inversion energy of triazasumanene is calculated to be 39.9 kcal/mol by DFT method at the B3LYP/6-311 + G(d,p) level. In contrast, the calculated values for **2** and **4** are 18.3 and 19.2 kcal/mol, respectively. This means that chiral triazasumanene **10** takes 1.1 billion years to racemize at 20 °C.

Both chiral derivatives of **9** and **10** exhibit the opposite Cotton effect curves (Figure 11), which are a mirror image of the corresponding enantiomers. The CD spectra of **9** and **10** demonstrated the existence of bowl chirality and remained intensive even after a week, indicative of a chiral memory effect. To measure the rate constant and bowl inversion energy of **9**, a racemization experiment was carried out at 488 K and analyzed by chiral HPLC. The racemization rate and energy of **9** were determined to be 1.24×10^{-6} s^{-1} (488 K) and 42.2 kcal/mol, respectively [12].

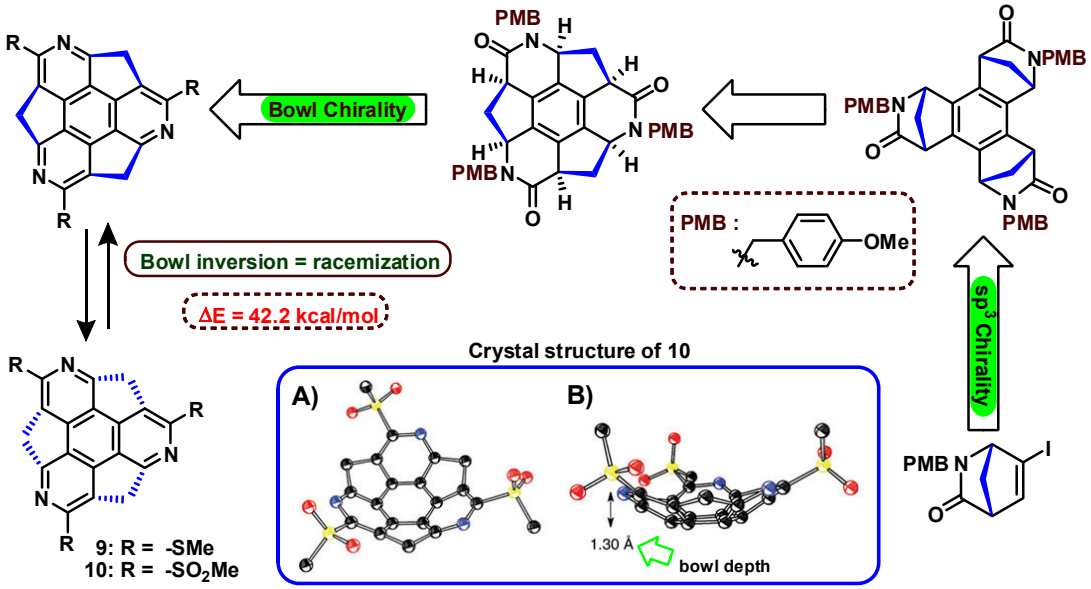

Scheme 3. Strategy for the asymmetric synthesis of chiral triazasumanene **9** and **10**; Insert: X-ray crystal ORTEP drawing structure of **10**; all hydrogen atoms omitted for clarity: (**A**) top view (with thermal ellipsoids set at 50% probability); (**B**) side view with bowl depth. Reprinted from [12]. © 2012 Nature Publishing Group.

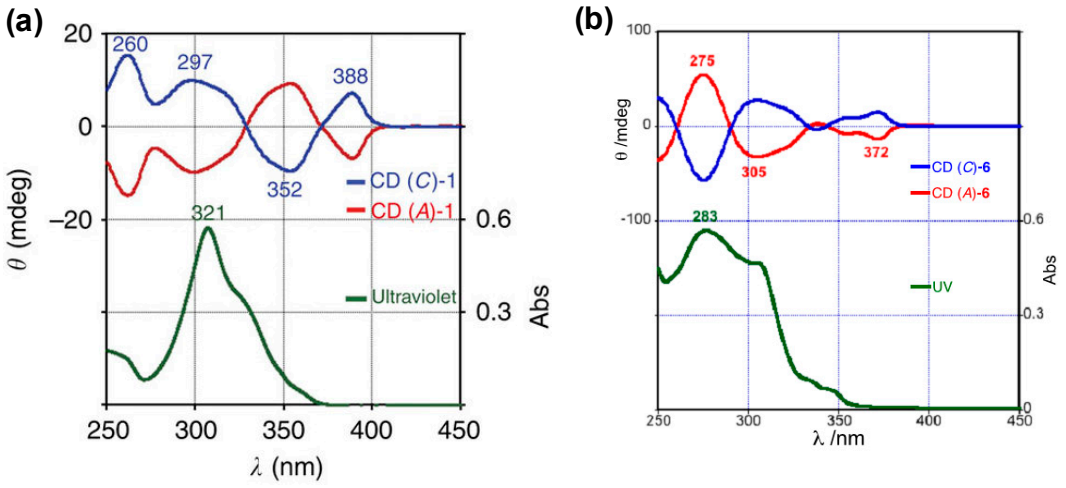

Figure 11. CD and ultraviolet/visible spectra of (**a**) compound **9** in CH_2Cl_2 solution (1.2×10^{-5} M). The blue line and red line are CD spectra of (*C*)-(−)-**9** and (*A*)-(+)-**9**, respectively; (**b**) Compound **10** in CH_2Cl_2 (5.0×10^{-5} M). The green line is an ultraviolet/visible spectrum. Reprinted from [12]. © 2012 Nature Publishing Group.

The above-discussed solution phase enantioselective synthesis of trimethylsumanene **4** and triazasumanene **9** and **10** represents a useful and versatile strategy for the construction of other homochiral curved π-electron systems from non-conjugated precursors. The chiral transmission from sp^3 stereogenic chirality to bowl chirality creates a new dimension for chiral-controlled 3D carbon materials like fullerene and CNTs.

7. Chiral Resolution of Buckybowls

The optical resolution of racemic chiral buckybowls has also been accomplished using derivatization method [13,71,78–81]. Derivatization at the outer rim of the buckybowl results in

a deeper bowl with high bowl inversion energy and makes it resolvable from its racemates using chiral HPLC [12,17,18]. The purity of enantio-enriched chiral buckybowls and its bowl chirality is mainly analyzed using CD spectroscopy, NMR, and chiral HPLC methods [82–87].

As shown above, **2** has less bowl inversion energy than **4**, and it undergoes much slower racemization at 0 °C ($t_{1/2}$ = 2 h) [17]. Based on this, Sakurai et al. reported the first asymmetric synthesis of chiral **4** [17], and the enantiomeric excess (*ee*) of **4** is determined by measuring the ^{1}H-NMR spectrum of **7**, which was derivatized from **4** using Mosher's acid chloride (Scheme 2) [17,18]. Upon introducing stereogenic centers at the sp^3 carbons at the benzylic positions, it became more stable and could be stored for a long time. The enantioselectivity of **6** was determined to be 89% *ee*, which matches the ^{1}H-NMR analysis of chiral derivatized compound **4** (90% *ee*). The chiral (*A*)-**6** buckybowl was eluted first with a retention time (t_R) of 38 min and another chiral buckybowl (*C*)-**6** was eluted later with a retention time of 42 min (Figure 12a). The separated enantiomers of buckybowl **6** were analyzed using CD spectroscopy, which showed the mirror image Cotton effect curves generated from its inherent bowl chirality (Figure 12b).

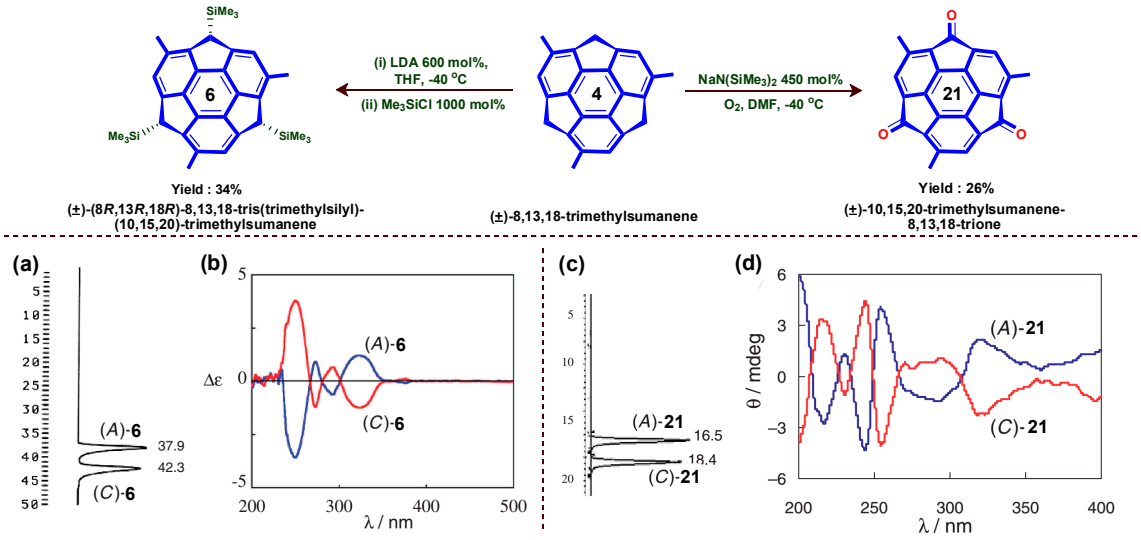

Figure 12. Synthesis of racemic (±)-**6** and (±)-**21** derivatives from racemic (±)-**4**. (**a**) Optical resolution of (±)-**6** by chiral HPLC (DAICEL CHIRALPAK IA, 2-propanol, retention time (t_R); 38 min for (*A*)-**6**, 42 min for (*C*)-**6**); (**b**) CD spectra of each enantiomers **6** in $CHCl_3$; (**c**) Optical resolution of (±)-**21** by chiral HPLC (DAICEL CHIRALPAK IA, hexane/2-propanol = 60/40, 9 °C, retention time (t_R); 17 min for (*A*)-**21**, 18 min for (*C*)-**21**); (**d**) CD spectra of enantioenriched **21** in CH_3CN at 27 °C. Blue line: CD spectra of (*A*)-**6** and (*A*)-**21**, respectively. Red line: CD spectra of (*C*)-**6** and (*C*)-**21**, respectively. Reprinted from [18]. © 2010 The Chemical Society of Japan.

Racemic (±)-**21** was prepared by aerobic oxidation of racemic (±)-**4** (Figure 12) [18]. The estimated bowl inversion energy of **21** was 23.5 kcal/mol, which corresponds to ca. 44 h half-life at 10 °C. Racemic (±)-**21** was optically resolved using a chiral HPLC (Figure 12c). The absolute configuration of each enantiomer was assigned based on the CD spectrum of the enantioenriched (*C*)-**21** prepared from (*C*)-**4**. The bowl chirality of the optically resolved enantioenriched buckybowls (*A*)- and (*C*)-**21** was analyzed using CD spectroscopy, which is shown in Figure 12d. In addition, the bowl inversion barrier of enantio-riched **21** was estimated to be 23.4 and 23.3 kcal/mol in CH_3CN and CH_2Cl_2, respectively, by measuring the time-dependent decay of the intensity of CD spectra at 255 nm at 30 °C [18]. These results led to the elucidation of the substituent effect and the correlation between bowl structure and bowl inversion energy [19].

Azasumanene **10** had a deeper bowl depth (1.30 Å) than **2** (1.10 Å) and showed extremely stable bowl chirality ($t_{1/2}$ = 54 billion years at 20 °C) because of its high bowl inversion energy

(ΔE = 42.2 kcal/mol) [12]. Similarly, C_3 symmetric chiral **8** was prepared by a Pd-catalyzed cross-coupling reaction between chiral **9** and (*p*-trifluoromethyl)phenyl boronic acid (Figure 13) [88]. The chirality of the obtained **8** was confirmed by chiral HPLC at 25 °C using a Daicel Chiralpak® IA column (Figure 13a,b). The CD and UV spectra were measured in a CH_2Cl_2 solution of enantioenriched **8** derivatives (Figure 13c), which shows the CD signals of the mirror image, indicating that the compounds are of opposite bowl chirality.

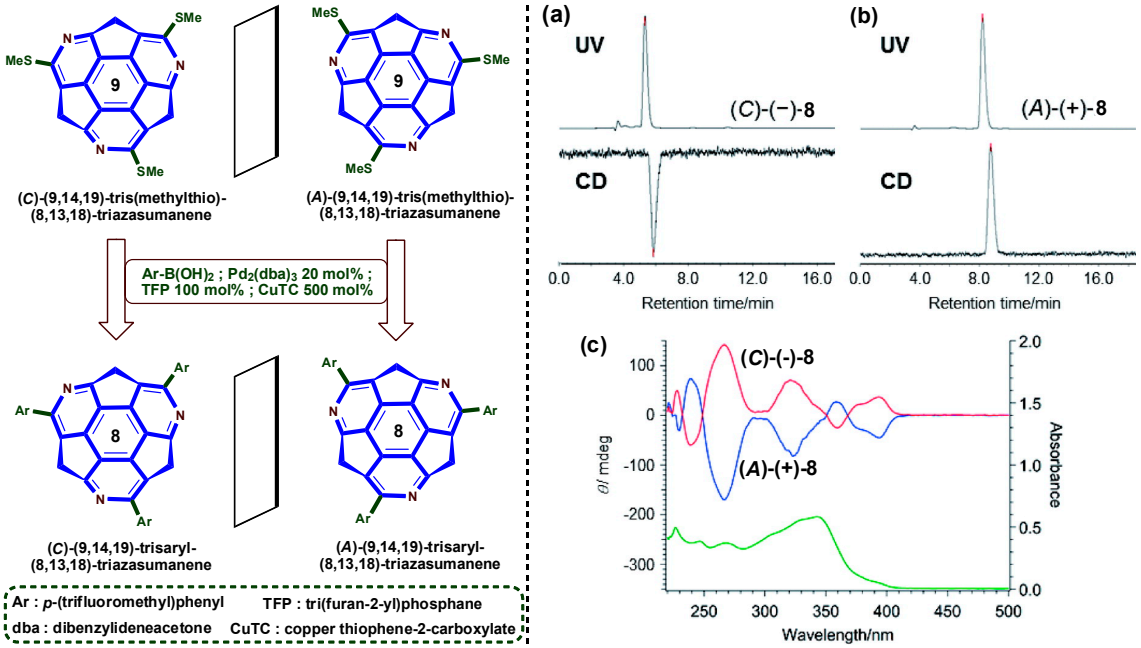

Figure 13. Strategy for the asymmetric synthesis of chiral **8** from chiral **9**: (**a**) HPLC chart of (*C*)-(−)-**8**; t_R = 5.31 min (UV) and 5.84 min (CD); (**b**) HPLC chart of (*A*)-(+)-**8**; t_R = 8.21 min (UV) and 8.76 min (CD). HPLC analysis was performed at 25 °C on a Daicel Chiralpak® IA column with hexane/CH_2Cl_2 = 50/50. Flow rate: 1 mL/min, detector wavelength: UV, 254 nm; CD, 270 nm; (**c**) CD and UV spectra of compound **8** in CH_2Cl_2 solution (1.5×10^{-5} M). Blue and red lines: CD spectra of (*A*)-(+)-**8** and (*C*)-(−)-**8**, respectively. Green line: UV spectrum of **8**. Reprinted from [88]. © 2017 The Chemical Society of Japan.

Recently, Yang and co-workers prepared azonia[*6*]helicene tethered with supramolecular host *β*-cyclodextrin, and used a chirality sensing probe for underivatized amino acids in water [89–94]. Indeed, tethered azonia[*6*]helicene acts as a conformationally robust chiral auxiliary to improve the chiral recognition ability of native cyclodextrins. Scott and co-workers successfully synthesized the first corannulene-[*n*]helicenes hybrids **22**–**25** by combining two classical nonplanar conjugated systems: the chiral bowl-shaped *π*-system, corannulene, and the helically chiral helicene (Figure 14). These compounds show unique molecular dynamics in their enantiomerization processes, including inversion motions of both the bowl and the helix [95].

Helix inversion renders *P* and *M* isomers, while corannulene bowl inversion results in concave and convex isomers, so it is predicted to have four isomers (convex-*P*, concave-*P*, convex-*M*, and concave-*M*) in equilibrium. Among the different conformers of corannulene-[*n*]helicenes, the conformer with a terminal helicene ring facing the convex surface of the bowl is more stable than the terminal ring facing the concave bowl surface, as the two forms display different degrees of steric congestion. For **22** and **23**, the energy barriers for bowl-to-bowl inversions were calculated to be 10.6 kcal/mol and 10.1 kcal/mol, respectively, and the helix inversions were 20.9 kcal/mol and 34.6 kcal/mol, respectively.

The enantiomers of corannulene-[*n*]helicenes hybrid were successfully resolved using a chiral-stationary-phase HPLC. The kinetics of thermal racemization of obtained conformers with

the *ee* of >99% was studied under different temperature, and the helix inversion barrier value of $\Delta G^{\ddagger}$ = 33.5 kcal/mol obtained experimentally is in consensus with the calculated one (34.6 kcal/mol) (Figure 14b). This hybrid system indicates that the chirality mainly arises from the rigid [6]helicene unit, and the non-rigid corannulene unit undergoes a rapid bowl-to-bowl inversion under ambient conditions.

The authors also synthesized **24** and **25** to study the different magnetic shielding effects of the convex and concave faces. The results show that the ring-current effect from the concave face of corannulene led to ^{1}H-NMR signal upfield shifts of 2 ppm to 5 ppm. However, the *t*-Bu group of **24** is shifted upfield by only 0.65 ppm compared to the *t*-Bu group in **25**, which is away from the convex face. This comparison demonstrates that the magnetic shielding of the concave face is much greater than that of the convex face. Similarly, various stereodynamic (non-rigid/fluctuating) systems **26**–**29** based on a corannulene bowl that possesses more than one stereogenic unit were synthesized and their selected diastereomeric conformers were studied via bowl-to-bowl inversion (Figure 14c) [57,96–98].

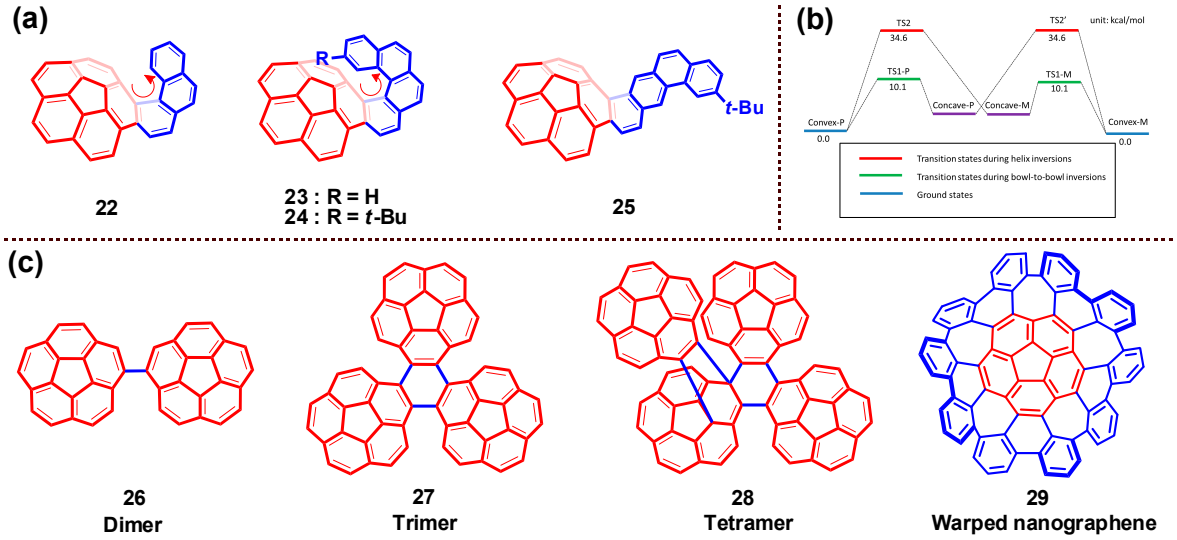

Figure 14. (**a**) Chemical structure of different chiral corannulene-[*n*]helicenes **22**–**25**; (**b**) Theoretical study of interconversion pathways of **23**. Relative Gibbs free energies (ΔG) were calculated at the B3LYP/6-31G(d) level at 298.15 K; (**c**) Structures of multiple corannulene derivatives **26**–**29**. (**b**) is reprinted from [95]. © 2016 American Chemical Society.

The enantiopure or enriched chiral buckybowls could be obtained by asymmetric synthesis or optical resolution of racemates using chiral HPLC. The enantiopure buckybowls with inherent chirality are expected to be applicable not only for asymmetric molecular recognition, novel chiral organic materials creation [15,24,39,99], and chiral ligands for transition metals, but also for precursors of chiral fullerenes and CNTs in chemical synthesis. Methods and approaches that control the bowl chirality can potentially be applied to the related chiral fullerenes and CNTs as well.

8. Chiral Metal Complexes of Buckybowls

In general, metals binding to π-conjugated compounds can be represented by the symbol η^{n} (n is the number of coordinating atoms). Fullerene and CNT and their derivatives form a coordination complex with various metal ion through their π-surfaces to form *exo*- as well as *endo*-hedral complexes, which have been used as a potential material in various fields such as molecular electronics and magnetic resonance imaging studies [100–102]. Interestingly, π-curved conjugated fragment **1** (bowl depth = 0.87 Å) preferentially coordinates with various metal ions in the convex surface in the η^{1}, η^{2}, and η^{6} modes [23,31,32,39,103–106]. Some corannulene derivatives form concave as well as convex face η^{6}-coordination complexes with ruthenium(II) [31,39,104]. Similarly, another C_{3v} symmetric,

curved π-conjugated bowl, **2**, forms coordination complexes through the η^1, η^2, η^4, η^5, and η^6 modes with limited transition metal ions [107].

In 2007, Hirao and co-workers reported the first selective concave-binding of $CpFe^+$ (Cp = C_5H_5) to **2** (Figure 15) [33]. The metalation of **2** was carried out in solvent-free conditions using ferrocene at 120 °C. Under the ligand exchange method with excesses of $CpFe^+$, the monometalated concave complex **30** was selectively afforded with a η^6 coordination (Figure 15a). In order to study the substituent effect, a methyl group was introduced into the cyclopentadiene ring, resulting in the concave selective complex **31** (Figure 15b). The bowl depth of **2** was not affected upon selective concave complexation of $CpFe^+$ (1.07–1.13 Å), whereas in $MeCpFe^+$ complexation the coordinatized side is flatted to 0.98 Å and the noncoordinated side was not affected (1.13 Å) (Figure 15a,b). Introduction of a chiral substituent *sec*-Bu to the Cp ring causes the target compound **32** as chiral (Figure 15c). The peaks of H_a split in ^{1}H-NMR due to the presence of a chiral *sec*-butyl group. Meanwhile, the concave-selective complexation was confirmed by the split of $H_{b\ endo}$. Furthermore, the chirality of complex **32** was proved by CD spectral analysis, which shows positive CD peaks at 272, 303, and 517 nm, respectively [34].

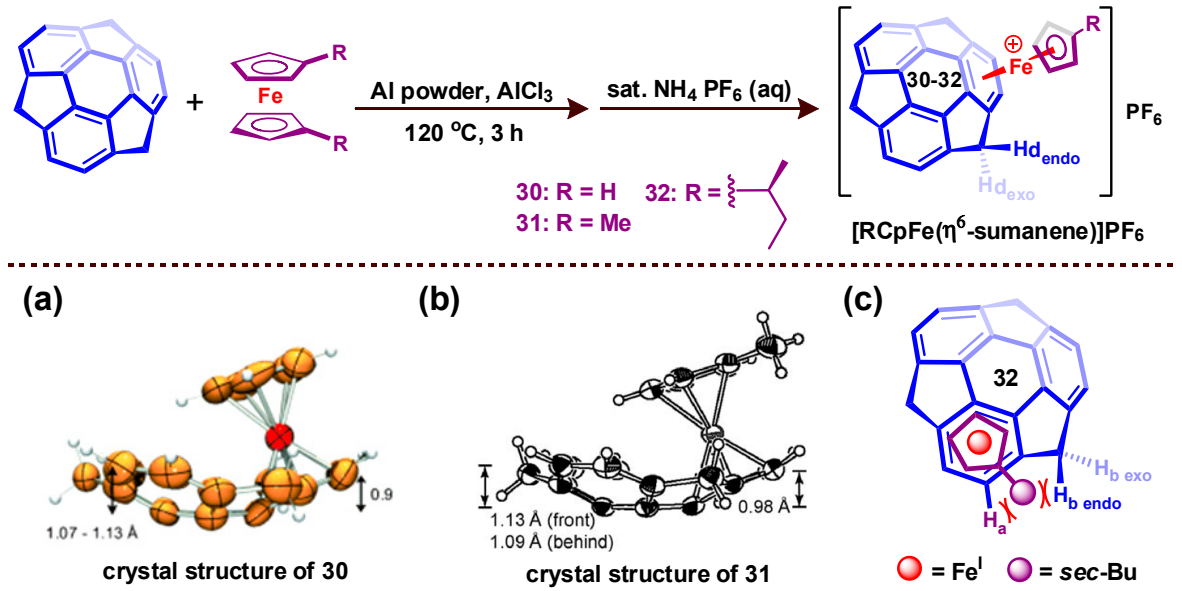

Figure 15. Synthetic strategy for the concave selective coordination complex formation of [RCpFe(sumanene)]PF_6. (**a**) Crystal structure of the cation of **30** with thermal ellipsoids set at 50% probability; side view with bowl depth; (**b**) Crystal structure of the cation of **31** with thermal ellipsoids set at 40% probability (the PF_6 ion and acetone are omitted for clarity), side view with bowl depth; (**c**) Schematic illustration of chiral concave-face selective coordination of sumanene. (**a**) is reprinted from [33], © 2007 Wiley-VCH Verlag GmbH & Co. KGaA, Weinheim; (**b**) is reprinted from [34], © 2009 Wiley-VCH Verlag GmbH & Co. KGaA, Weinheim.

Four years later, the first chiral selective convex-face complex based on pentasubstituted C_5-symmetric bowl corannulene was reported by Siegel and co-workers [36]. Four kinds of compounds were synthesized to investigate the effect of different substituents in bicyclo[2.2.1]hepta-2,5-diene (nbd) and corannulene derivatives (R = H, Me and *t*-Bu). The crystal structure of **34** is given in Figure 16a. From the stereochemical analysis, **35** and **36** were predicted to have diastereomers **35a**/**35b** pair and **36a**/**36b** pair, respectively, arising from the rotation of chiral nbd ligand (Figure 16b). The complex is more likely to yield a static form with the steric repulsion between nbd ligand and corannulene. The calculated energy gaps between **35a**/**35b** pair and **36a**/**36b** pair are 1.88 kcal/mol and 3.54 kcal/mol, respectively. However, **35a**/**35b** was observed with a ratio of 2.5:1, while only **36a** was detected in the latter pair. These phenomena confirmed the hypothesis that the complex tends to exist in the static form with the steric hindrance.

The Cotton effects of **33** and **36** were observed in the CD spectra and confirmed the steric repulsion hypothesis. The distinct bathochromic shift of **33** and **36** compared to the free chiral nbd ligand was ascribed to the electron transfer from nbd ligand to the corannulene. This kind of curved π-bowl chiral complexation has the potential to function as a catalyst in asymmetrical organometallic chemistry and promote the understanding of selective π-bowl coordination.

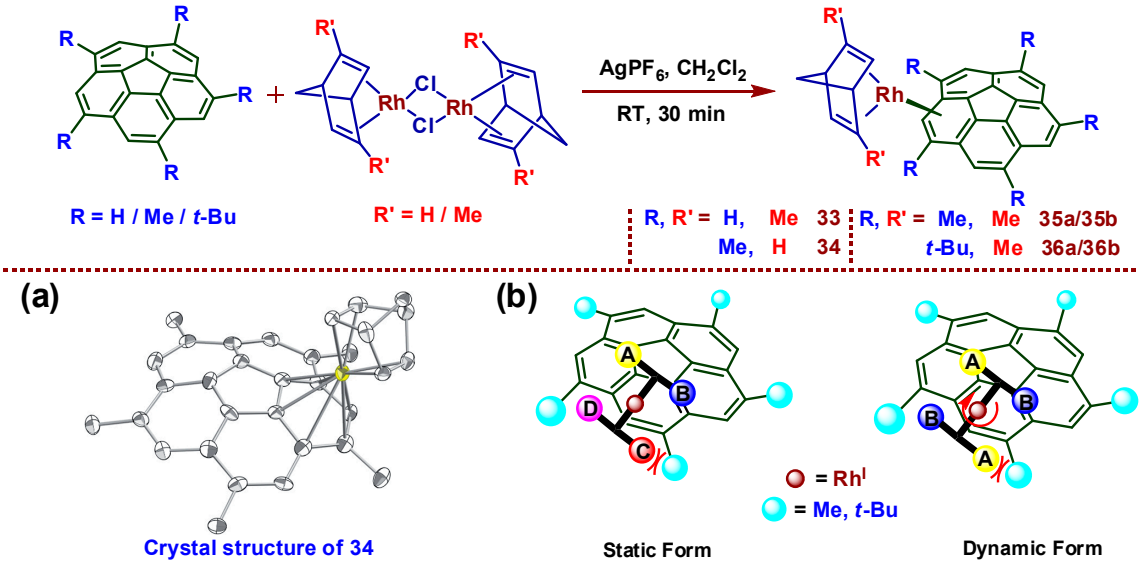

Figure 16. Synthesis route of selective C_5-symmetric corannulene-based convex-face complexes **33**–**36**: (**a**) X-ray crystal structure of **34**; (**b**) schematic illustration of diastereomers due to steric repulsion from rotation of the fragment. (**a**) is reprinted from [36], © 2011 Wiley-VCH Verlag GmbH & Co. KGaA, Weinheim.

9. Chiral Assembly of Buckybowls

Generally, various cyclic systems have inherent chirality because of their conformational stability and rigidity, which make them useful as chiroptical sensing probes [108–110]. Their preorganized binding sites can recognize optically active molecular species selectively via noncovalent interactions and gave a conformationally stable chiral organic structures. Furthermore, essential molecular chiral components amplify to form 3D supramolecularly assembled architectures and oriented nanoscale assemblies [111,112]. The nanoscale chirality of these 3D chiral supramolecular assemblies has potential application in functional soft materials.

Curved π-conjugated buckybowl corannulenes mainly form noncolumnar structures through a CH–π interaction rather than a π–π stacking interaction [28–30]. C_5-Symmetric corannulene undergoes rapid bowl-to-bowl inversion/racemization at ambient or even low temperatures, and is unable to resolve into their enantiomers. Aida and co-workers reported a C_{5v}-symmetric decasubstituted liquid crystalline (LC) corannulene derivative tethered with thioalkyl-amide-tribranched paraffinic side chains that forms self-assembled hexagonal columnar LC structures [3]. The nonpolar corannulene derivative can align homeotropically to the electrode surface with an applied electric field, and the alignment of corannulene was memorized for a long time. Hydrogen bond formation among the amide groups plays a key role in the formation of LC.

In order to resolve their enantiomers, the substituents were appended at the outer rim of corannulene viz. thioalkyl chains and amide groups (Figure 17A) [21]. C_5-symmetric corannulene-based chiral initiators and monomers carrying amide-appended thioalkyl side chains were synthesized from 1,3,5,7,9-pentachlorocorannulene according to methods analogous to those reported by Scott and co-workers [113]. The amide derivatives form a unimolecular closed cage

through "intramolecular" H-bonding interactions, which represents the first unimolecular host that is responsive to the chiral hydrocarbon solvent and obeys the majority rule in a chiral environment.

Non-amide derivative **37** does not show chiroptical activity even in chiral limonene, and no CD signal could be seen for $\mathbf{38}_R$ despite a chiral center in the side chain, whereas amide derivative **40M** showed chiroptical activity in the presence of chiral limonene. Compounds $\mathbf{41M}_R$ and $\mathbf{41M}_S$, in which amide linkers at the periphery of corannulene are attached to a chiral side chain, show chiroptical activity even in the achiral solvents. The computational simulation studies suggested that the formed stereoisomeric unimolecular closed cages exist in four equilibrated structures (Figure 17B). These amide derivatives form four kinds of "intramolecular" closed cages, and its cyclic amide H-bonded networks take clockwise and anticlockwise geometries. The corannulene bowl chirality axis and the direction of the intramolecular H-bonding (C=O $\cdots$ H-N) network rotate in the same clockwise or anticlockwise directions (denoted as AA and CC); $\mathbf{39}_{\mathbf{AA}}$ and $\mathbf{39}_{\mathbf{CC}}$ structures are more stable and energetically favored than different directions (denoted as AC and CA; $\mathbf{39}_{\mathbf{AC}}$ and $\mathbf{39}_{\mathbf{CA}}$).

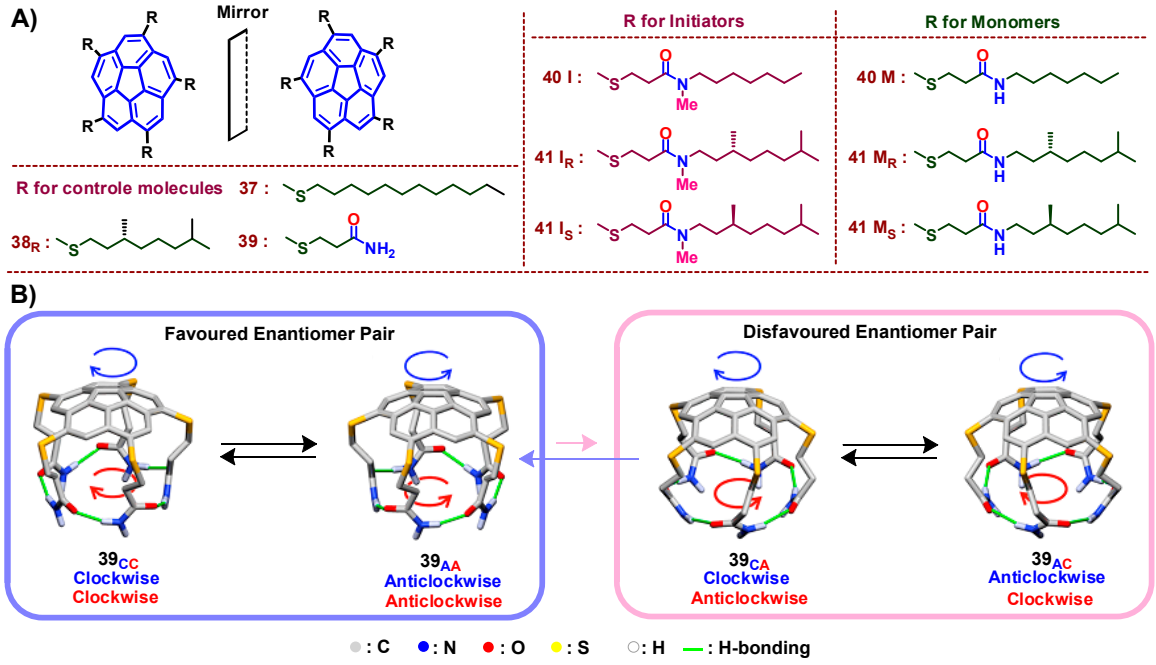

Figure 17. (**A**) Chemical structures of C_5-symmetric corannulene derivatives **37**–**41** bearing chiral or achiral side chains; (**B**) Schematic representations of the bowl inversion equilibrium using simplified molecular model **39** for C_5-symmetric corannulenes carrying thioalkyl side chains featuring intramolecularly H-bonded amide units. Blue- and red-colored arc-shaped arrows represent the directions of H→SR and H-bonded N-H→O=C arrays, respectively, along the corannulene periphery. Subscripts C and A for **39** denote the clockwise and anticlockwise directions (tentatively defined), respectively. Four possible stereoisomers were energy minimized at the SCS-MP2/def2-TZVPP//DFT-D3-TPSS/defTZVP level. (**B**) is reprinted from [21]. © 2014 American Chemical Society.

The compound **40M** exhibited opposite Cotton effect curves in chiral solvents (*S*)-limonene and (*R*)-limonene, respectively. Likewise, chiral $\mathbf{41M_R}/\mathbf{41M_S}$ showed chiroptical activity even in an achiral solvent such as methylcyclohexane, displaying mutually mirror-imaged CD spectra (Figure 18a). However, upon addition of a protonic solvent like ethanol, which is known to deteriorate the H-bonding, the $\mathbf{41M_R}/\mathbf{41M_S}$ became CD-silent due to the breaking of the intramolecular H-bonding network. In methylcyclohexane, the CD spectral change of **40M** was monitored in a wide temperature range from −40 to 40 °C. When the temperature is lowered to −40 °C, the %*de* of **40M** is increased to 45%. At 20 °C, %*de* of $\mathbf{41M_R}$ is enhanced to 80% when (*R*)-limonene was used as the solvent, whereas

41M$_R$ becomes CD-silent when (*S*)-limonene is used as the solvent (Figure 18b). A similar trend is followed by **41M$_S$** (Figure 18b), which indicates that the chiral side-chain of **40M** could cooperate with the chiral solvent, either positively or negatively, in desymmetrizing the bowl inversion equilibrium of the corannulene core. A sigmoidal signal was observed in the CD spectra which demonstrated that the majority rule works in the unimolecular system [21].

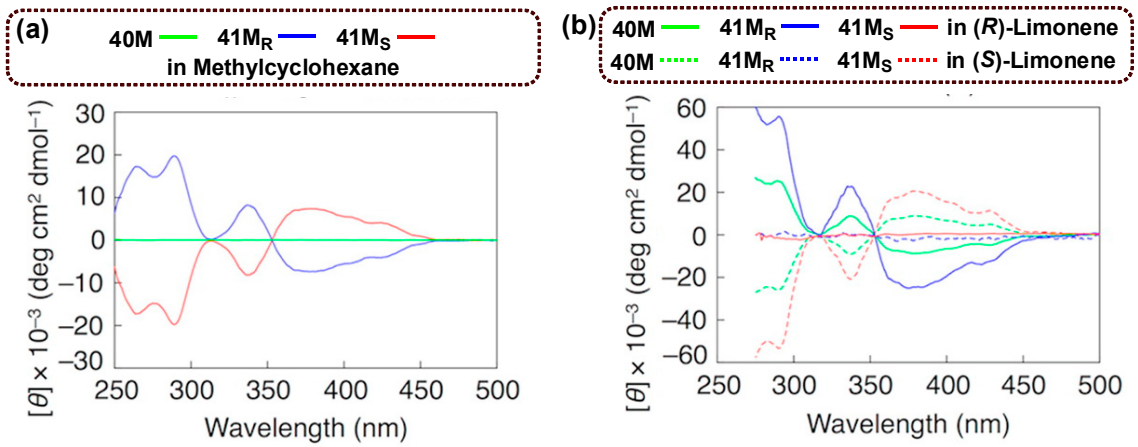

Figure 18. Circular dichroism (CD) spectra at 20 °C of **40M** (green), **41M$_R$** (blue), and **41M$_S$** (red) (20 μM) in (**a**) methylcyclohexane and (**b**) (*R*)- (solid curves) and (*S*)-limonene (dashed curves). Reprinted from [21]. © 2014 American Chemical Society.

Inspired by the metastable property of corannulene derivative **40M**, Aida and co-workers came up with an ingenious strategy to achieve the first example of chiral chain-growth supramolecular polymerization [8]. To break the intramolecular H-bonding network of **40M**, they replaced the H atom connected in N with a methyl group and used **40I** as an initiator of supramolecular polymerization. The carbonyl group of the initiator can function as an H-bonding acceptor, thus attacking the monomer via H-bonding. Subsequently, the self-opening monomer can act as an initiator using its own free C=O, resulting in an oligomer **I-[M]$_2$** with the free C=O end capped as well (Figure 19). As the oligomer elongates, the first chain-growth supramolecular polymerization is realized. Surprisingly, the chiral chain-growth polymerization can also be achieved via chiral initiator **41I$_R$**/**41I$_S$**. When chiral initiator **41I$_S$** was added with racemic monomers **41M$_R$** and **41M$_S$**, chiral helical assemblies were achieved from the analysis of size-exclusion chromatography (SEC), meaning that only **41M$_S$** can polymerize. As a result, chiral resolution of **41M$_R$** and **41M$_S$** was also realized successfully in the same way [8].

Differing from the classical chiral assembly formation in a macroscopic organic system, chiral microscopic assemblies of buckybowl hemifullerene at the surface of inorganic crystal were achieved by Fasel and co-workers [114]. They discovered how chiral bowl-shape hemifullerenes, derivatives of sumanene (Figure 20A), restructure on the copper surface atoms into chiral structures such as chiral nanowires and chiral islands. Unlike other researchers using polar molecules with carbonyl groups as chiral surface modifiers [115,116], Fasel et al. [114] turned their attention to metal-aromatic coordination bonds and found hemifullerenes suitable to induce chirality on a copper surface. Surprisingly, *M* enantiomers of hemifullerenes align along the [$\bar{3}3\bar{4}$] direction, creating R kinks, while *P* counterparts align along the [$\bar{3}34$] direction, forming S kinks, which differs from the previously reported arrangement of C_{60}/corannulene along the Cu[110] direction [2]. This phenomenon is observed via scanning tunneling microscopy (STM) at 50 K and X-ray photoelectron diffraction (XPD) at room temperature. The optimized adsorption configuration was simulated by DFT, revealing that the creation of chiral kink creation can be explained by a three-point contact model, which is three η^1-coordinated Cu–C bonds at this point.

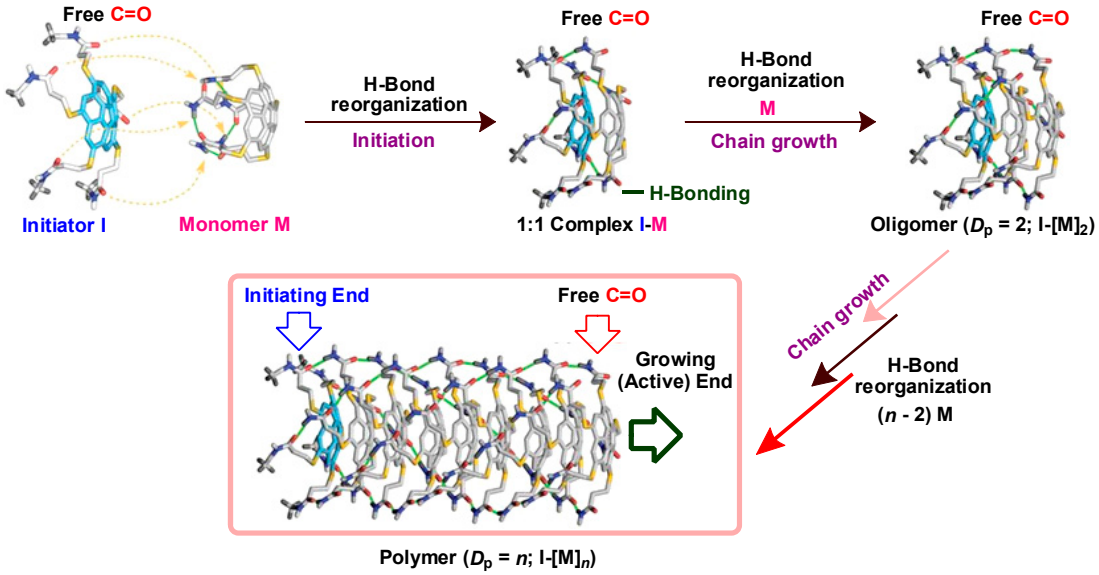

Figure 19. Schematic representations of the chiral chain-growth supramolecular polymerization of chiral pentasubstituted corannulene derivative. Reprinted from [8]. © 2015 Science American Association for the Advancement of Science (AAAS).

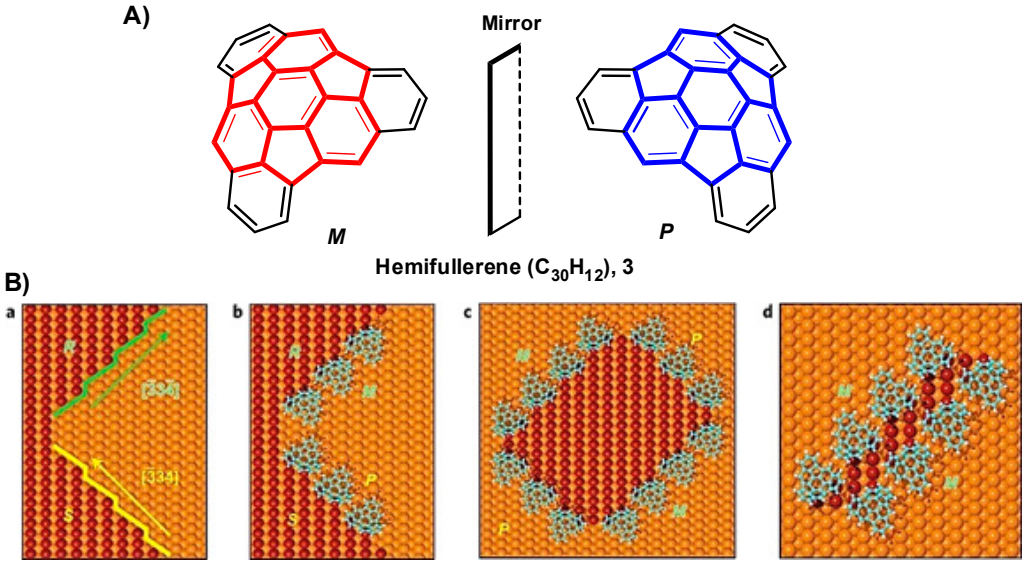

Figure 20. (**A**) Chemical structure of hemifullerene **3** enantiomers; (**B**) a. Structural model of the observed step edge with alternating [$\bar{3}3\bar{4}$] and [$\bar{3}34$] segments and the formation of chiral kink sites; b. structural model of R kinks decorated by *M* enantiomers and S kinks decorated by *P* enantiomers; c. structural model of a chiral island stabilized by hemifullerene enantiomers; d. structural model of a chiral Cu nanowire stabilized by *M*-hemifullerene along the [$\bar{3}3\bar{4}$] direction. Reprinted from [114]. © 2010 Nature Publishing Group.

Furthermore, the chiral island and nanowire (Figure 20B) were found to form with different alignments of hemifullerenes. The results indicate the emergence of a chiral shape on Cu surface is of great importance to help investigate the elementary mechanism of chiral recognition or induction occurring on an achiral crystal surface. Unfortunately, efforts to separate the enantiomers adsorbed on the Cu surface were not successful [114].

Tethering the various alkyl chains with different length, number, substitution position, and nature of chiral carbons to the outer rim π-conjugated buckybowls is an effective way to tune the

chiral assembly formation, the function of the system and their soft materialization. Extension of π-conjugation through the outer rim of the corannulene provided a single chiral CNT [114].

10. Conclusions and Outlook

In conclusion, this review summarizes the recent progress of studies on the bowl chirality, focusing on the two kinds of buckybowl compounds, corannulenes and sumanenes. These buckybowls possess curved aromatic rings, and introducing substituents on their aromatic periphery results in the loss of planar symmetry to generate a unique kind of chirality, so-called bowl chirality. The curved aromatic surface is possibly flipped, and such a bowl-to-bowl inversion causes switching of the bowl chirality. The size and shape of the substituents, a doped heteroatom in the aromatic bowl, and introducing a metal complex on the surface of buckybowls will significantly influence the bowl-to-bowl inversion energy as well as the racemization rate. Enantio-/diastereo- pure/enriched chiral buckybowls could be obtained by chiral resolution or chiral synthesis. The introduction of a chiral chain to the rim of the buckybowl dominated the asymmetric synthesis of chiral buckybowls. Sumanene **2** usually has higher bowl-to-bowl inversion energy than corannulene **1**, and asymmetric synthesis of chiral trimethylsumanene **4** and triazasumanene **9** and **10** has been realized using chiral non-conjugated precursors. The selective chiral assemblies of buckybowls with unique chemical and electronic properties may contribute to the development of the field of electronic devices and energy storage. In addition, the synthesis of homochiral CNTs continuously attracts scientists and chiral buckybowls may open up new opportunities in this area. The chiral assemblies of buckybowls are attractive, in relation to topics such as chiral amplification, chiral induction, and chiral memory. There is no doubt that the study of chiral buckybowls is still immature yet highly promising; further investigation will provide more insight into this particular area and lead to applications in various fields such as materials, electronics, and photonics.

Acknowledgments: We acknowledge the National Natural Science Foundation of China (Nos. 21572142, 21402129, 21372165, 31370735, and 21321061), the National Key Research and Development Program of China (grant No. 2017YFA0505900), and the State Key Laboratory of Fine Chemicals (KF 1508) and Sichuan Province Science Foundation for Youths (No. 2015JQ0029) for financial support.

Author Contributions: Kuppusamy Kanagaraj, Kangjie Lin, Wanhua Wu, Guowei Gao, Zhihui Zhong, Dan Su and Cheng Yang collected and analyzed the references and data and wrote the paper.

Conflicts of Interest: The authors declare no conflict of interest.

References

1. Shi, K.; Lei, T.; Wang, X.-Y.; Wang, J.-Y.; Pei, J. A bowl-shaped molecule for organic field-effect transistors: Crystal engineering and charge transport switching by oxygen doping. *Chem. Sci.* **2014**, *5*, 1041–1045. [CrossRef]
2. Xiao, W.; Passerone, D.; Ruffieux, P.; Aït-Mansour, K.; Gröning, O.; Tosatti, E.; Siegel, J.S.; Fasel, R. C60/corannulene on Cu(110): A surface-supported bistable buckybowl-buckyball host-guest system. *J. Am. Chem. Soc.* **2008**, *130*, 4767–4771. [CrossRef] [PubMed]
3. Miyajima, D.; Tashiro, K.; Araoka, F.; Takezoe, H.; Kim, J.; Kato, K.; Takata, M.; Aida, T. Liquid crystalline corannulene responsive to electric field. *J. Am. Chem. Soc.* **2009**, *131*, 44–45. [CrossRef] [PubMed]
4. Lovas, F.J.; McMahon, R.J.; Grabow, J.-U.; Schnell, M.; Mack, J.; Scott, L.T.; Kuczkowski, R.L. Interstellar chemistry: A strategy for detecting polycyclic aromatic hydrocarbons in space. *J. Am. Chem. Soc.* **2005**, *127*, 4345–4349. [CrossRef] [PubMed]
5. Zhang, L.; Qin, L.; Wang, X.; Cao, H.; Liu, M. Supramolecular chirality in self-assembled soft materials: Regulation of chiral nanostructures and chiral functions. *Adv. Mater.* **2014**, *26*, 6959–6964. [CrossRef] [PubMed]
6. Li, X.; Kang, F.; Inagaki, M. Buckybowls: Corannulene and its derivatives. *Small* **2016**, *12*, 3206–3223. [CrossRef] [PubMed]
7. Amaya, T.; Hirao, T. Chemistry of sumanene. *Chem. Rec.* **2015**, *15*, 310–321. [CrossRef] [PubMed]

8. Kang, J.; Miyajima, D.; Mori, T.; Inoue, Y.; Itoh, Y.; Aida, T. A rational strategy for the realization of chain-growth supramolecular polymerization. *Science* **2015**, *347*, 646–651. [CrossRef] [PubMed]
9. Higashibayashi, S.; Sakurai, H. Synthesis of sumanene and related buckybowls. *Chem. Lett.* **2011**, *40*, 122–128. [CrossRef]
10. Scott, L.T.; Jackson, E.A.; Zhang, Q.; Steinberg, B.D.; Bancu, M.; Li, B. A short, rigid, structurally pure carbon nanotube by stepwise chemical synthesis. *J. Am. Chem. Soc.* **2012**, *134*, 107–110. [CrossRef] [PubMed]
11. Hembury, G.A.; Borovkov, V.V.; Inoue, Y. Chirality-sensing supramolecular systems. *Chem. Rev.* **2008**, *108*, 1–73. [CrossRef] [PubMed]
12. Tan, Q.; Higashibayashi, S.; Karanjit, S.; Sakurai, H. Enantioselective synthesis of a chiral nitrogen-doped buckybowl. *Nat. Commun.* **2012**, *3*, 891. [CrossRef] [PubMed]
13. Scott, L.T.; Hashemi, M.M.; Bratcher, M.S. Corannulene bowl-to-bowl inversion is rapid at room temperature. *J. Am. Chem. Soc.* **1992**, *114*, 1920–1921. [CrossRef]
14. Seiders, T.J.; Baldridge, K.K.; Grube, G.H.; Siegel, J.S. Structure/energy correlation of bowl depth and inversion barrier in corannulene derivatives: Combined experimental and quantum mechanical analysis. *J. Am. Chem. Soc.* **2001**, *123*, 517–525. [CrossRef] [PubMed]
15. Amaya, T.; Sakane, H.; Muneishi, T.; Hirao, T. Bowl-to-bowl inversion of sumanene derivatives. *Chem. Commun.* **2008**, 765–767. [CrossRef]
16. Hayama, T.; Baldridge, K.K.; Wu, Y.-T.; Linden, A.; Siegel, J.S. Steric isotope effects gauged by the bowl-inversion barrier in selectively deuterated pentaarylcorannulenes. *J. Am. Chem. Soc.* **2008**, *130*, 1583–1591. [CrossRef] [PubMed]
17. Higashibayashi, S.; Sakurai, H. Asymmetric synthesis of a chiral buckybowl, trimethylsumanene. *J. Am. Chem. Soc.* **2008**, *130*, 8592–8593. [CrossRef] [PubMed]
18. Tsuruoka, R.; Higashibayashi, S.; Ishikawa, T.; Toyota, S.; Sakurai, H. Optical resolution of chiral buckybowls by chiral HPLC. *Chem. Lett.* **2010**, *39*, 646–647. [CrossRef]
19. Higashibayashi, S.; Tsuruoka, R.; Soujanya, Y.; Purushotham, U.; Sastry, G.N.; Seki, S.; Ishikawa, T.; Toyota, S.; Sakurai, H. Trimethylsumanene: Enantioselective synthesis, substituent effect on bowl structure, inversion energy, and electron conductivity. *Bull. Chem. Soc. Jpn.* **2012**, *85*, 450–467. [CrossRef]
20. Shrestha, B.B.; Karanjit, S.; Higashibayashi, S.; Sakurai, H. Correlation between bowl-inversion energy and bowl depth in substituted sumanenes. *Pure Appl. Chem.* **2014**, *86*, 747–753. [CrossRef]
21. Kang, J.; Miyajima, D.; Itoh, Y.; Mori, T.; Tanaka, H.; Yamauchi, M.; Inoue, Y.; Harada, S.; Aida, T. C5-symmetric chiral corannulenes: Desymmetrization of bowl inversion equilibrium via "intramolecular" hydrogen-bonding network. *J. Am. Chem. Soc.* **2014**, *136*, 10640–10644. [CrossRef] [PubMed]
22. Juríček, M.; Strutt, N.L.; Barnes, J.C.; Butterfield, A.M.; Dale, E.J.; Baldridge, K.K.; Stoddart, J.F.; Siegel, J.S. Induced-fit catalysis of corannulene bowl-to-bowl inversion. *Nat. Chem.* **2014**, *6*, 222–228. [CrossRef] [PubMed]
23. Seiders, T.J.; Baldridge, K.K.; O'Connor, J.M.; Siegel, J.S. Hexahapto metal coordination to curved polyaromatic hydrocarbon surfaces: The first transition metal corannulene complex. *J. Am. Chem. Soc.* **1997**, *119*, 4781–4782. [CrossRef]
24. Sakurai, H.; Daiko, T.; Sakane, H.; Amaya, T.; Hirao, T. Structural elucidation of sumanene and generation of its benzylic anions. *J. Am. Chem. Soc.* **2005**, *127*, 11580–11581. [CrossRef] [PubMed]
25. Shrestha, B.B.; Morita, Y.; Kojima, T.; Kawano, M.; Higashibayashi, S.; Sakurai, H. Eclipsed columnar packing in crystal structure of sumanenetrione. *Chem. Lett.* **2014**, *43*, 1294–1296. [CrossRef]
26. Sygula, A.; Yanney, M.; Henry, W.P.; Fronczek, F.R.; Zabula, A.V.; Petrukhina, M.A. Inclusion complexes and solvates of buckycatcher, a versatile molecular host with two corannulene pincers. *Cryst. Growth Des.* **2014**, *14*, 2633–2639. [CrossRef]
27. Yamada, M.; Ohkubo, K.; Shionoya, M.; Fukuzumi, S. Photoinduced electron transfer in a charge-transfer complex formed between corannulene and li+@C60 by concave–convex π–π interactions. *J. Am. Chem. Soc.* **2014**, *136*, 13240–13248. [CrossRef] [PubMed]
28. Merz, L.; Parschau, M.; Zoppi, L.; Baldridge, K.K.; Siegel, J.S.; Ernst, K.-H. Reversible phase transitions in a buckybowl monolayer. *Angew. Chem. Int. Ed.* **2009**, *48*, 1966–1969. [CrossRef] [PubMed]
29. Bauert, T.; Merz, L.; Bandera, D.; Parschau, M.; Siegel, J.S.; Ernst, K.-H. Building 2d crystals from 5-fold-symmetric molecules. *J. Am. Chem. Soc.* **2009**, *131*, 3460–3461. [CrossRef] [PubMed]

30. Liu, Y.-M.; Xia, D.; Li, B.-W.; Zhang, Q.-Y.; Sakurai, T.; Tan, Y.-Z.; Seki, S.; Xie, S.-Y.; Zheng, L.-S. Functional sulfur-doped buckybowls and their concave–convex supramolecular assembly with fullerenes. *Angew. Chem. Int. Ed.* **2016**, *55*, 13047–13051. [CrossRef] [PubMed]
31. Vecchi, P.A.; Alvarez, C.M.; Ellern, A.; Angelici, R.J.; Sygula, A.; Sygula, R.; Rabideau, P.W. Synthesis and structure of a dimetallated buckybowl: Coordination of one {cp*ru}+ unit to each side of corannulene. *Angew. Chem. Int. Ed.* **2004**, *43*, 4497–4500. [CrossRef] [PubMed]
32. Petrukhina, M.A.; Andreini, K.W.; Peng, L.; Scott, L.T. Hemibuckminsterfullerene C30H12: X-ray crystal structures of the parent hydrocarbon and of the two-dimensional organometallic network {[Rh2(O2CCF3)4]3(C30H12)}. *Angew. Chem. Int. Ed.* **2004**, *43*, 5477–5481. [CrossRef] [PubMed]
33. Amaya, T.; Sakane, H.; Hirao, T. A concave-bound cpfe complex of sumanene as a metal in a π-bowl. *Angew. Chem. Int. Ed.* **2007**, *46*, 8376–8379. [CrossRef] [PubMed]
34. Sakane, H.; Amaya, T.; Moriuchi, T.; Hirao, T. A chiral concave-bound cyclopentadienyl iron complex of sumanene. *Angew. Chem. Int. Ed.* **2009**, *48*, 1640–1643. [CrossRef] [PubMed]
35. Amaya, T.; Wang, W.-Z.; Sakane, H.; Moriuchi, T.; Hirao, T. A dynamically inverting π-bowl complex. *Angew. Chem. Int. Ed.* **2010**, *49*, 403–406. [CrossRef] [PubMed]
36. Bandera, D.; Baldridge, K.K.; Linden, A.; Dorta, R.; Siegel, J.S. Stereoselective coordination of C5-symmetric corannulene derivatives with an enantiomerically pure [rhi(nbd*)] metal complex. *Angew. Chem. Int. Ed.* **2011**, *50*, 865–867. [CrossRef] [PubMed]
37. Amaya, T.; Seki, S.; Moriuchi, T.; Nakamoto, K.; Nakata, T.; Sakane, H.; Saeki, A.; Tagawa, S.; Hirao, T. Anisotropic electron transport properties in sumanene crystal. *J. Am. Chem. Soc.* **2009**, *131*, 408–409. [CrossRef] [PubMed]
38. Schmidt, B.M.; Seki, S.; Topolinski, B.; Ohkubo, K.; Fukuzumi, S.; Sakurai, H.; Lentz, D. Electronic properties of trifluoromethylated corannulenes. *Angew. Chem. Int. Ed.* **2012**, *51*, 11385–11388. [CrossRef] [PubMed]
39. Wu, Y.-T.; Siegel, J.S. Aromatic molecular-bowl hydrocarbons: Synthetic derivatives, their structures, and physical properties. *Chem. Rev.* **2006**, *106*, 4843–4867. [CrossRef] [PubMed]
40. Tsefrikas, V.M.; Scott, L.T. Geodesic polyarenes by flash vacuum pyrolysis. *Chem. Rev.* **2006**, *106*, 4868–4884. [CrossRef] [PubMed]
41. Amaya, T.; Hirao, T. A molecular bowl sumanene. *Chem. Commun.* **2011**, *47*, 10524–10535. [CrossRef] [PubMed]
42. Sygula, A. Chemistry on a half-shell: Synthesis and derivatization of buckybowls. *Eur. J. Org. Chem.* **2011**, *2011*, 1611–1625. [CrossRef]
43. Filatov, A.S.; Petrukhina, M.A. Probing the binding sites and coordination limits of buckybowls in a solvent-free environment: Experimental and theoretical assessment. *Coord. Chem. Rev.* **2010**, *254*, 2234–2246. [CrossRef]
44. Zoppi, L.; Martin-Samos, L.; Baldridge, K.K. Structure–property relationships of curved aromatic materials from first principles. *Acc. Chem. Res.* **2014**, *47*, 3310–3320. [CrossRef] [PubMed]
45. Sanchez-Valencia, J.R.; Dienel, T.; Groning, O.; Shorubalko, I.; Mueller, A.; Jansen, M.; Amsharov, K.; Ruffieux, P.; Fasel, R. Controlled synthesis of single-chirality carbon nanotubes. *Nature* **2014**, *512*, 61–64. [CrossRef] [PubMed]
46. Sekiguchi, R.; Kudo, S.; Kawakami, J.; Sakai, A.; Ikeda, H.; Nakamura, H.; Ohta, K.; Ito, S. Preparation of a cyclic polyphenylene array for a chiral-type carbon nanotube segment. *Bull. Chem. Soc. Jpn.* **2016**, *89*, 1260–1275. [CrossRef]
47. Liu, B.; Wu, F.; Gui, H.; Zheng, M.; Zhou, C. Chirality-controlled synthesis and applications of single-wall carbon nanotubes. *ACS Nano* **2017**, *11*, 31–53. [CrossRef] [PubMed]
48. Brandt, J.R.; Salerno, F.; Fuchter, M.J. The added value of small-molecule chirality in technological applications. *Nat. Rev. Chem.* **2017**, *1*, 0045. [CrossRef]
49. Yang, C.; Inoue, Y. Supramolecular photochirogenesis. *Chem. Soc. Rev.* **2014**, *43*, 4123–4143. [CrossRef] [PubMed]
50. Yang, C.; Ke, C.; Liang, W.; Fukuhara, G.; Mori, T.; Liu, Y.; Inoue, Y. Dual supramolecular photochirogenesis: Ultimate stereocontrol of photocyclodimerization by a chiral scaffold and confining host. *J. Am. Chem. Soc.* **2011**, *133*, 13786–13789. [CrossRef] [PubMed]
51. Fan, C.; Wu, W.; Chruma, J.J.; Zhao, J.; Yang, C. Enhanced triplet-triplet energy transfer and upconversion fluorescence through host-guest complexation. *J. Am. Chem. Soc.* **2016**, *138*, 15405. [CrossRef] [PubMed]

52. Xiao, C.; Zhao, W.-Y.; Zhou, D.-Y.; Huang, Y.; Tao, Y.; Wu, W.-H.; Yang, C. Recent advance of photochromic diarylethenes-containing supramolecular systems. *Chin. Chem. Lett.* **2015**, *26*, 817–824. [CrossRef]
53. Yang, C. Recent progress in supramolecular chiral photochemistry. *Chin. Chem. Lett.* **2013**, *24*, 437–441. [CrossRef]
54. Thilgen, C.; Diederich, F. Structural aspects of fullerene chemistrya journey through fullerene chirality. *Chem. Rev.* **2006**, *106*, 5049–5135. [CrossRef] [PubMed]
55. Cahn, R.S.; Ingold, C.; Prelog, V. Specification of molecular chirality. *Angew. Chem. Int. Ed.* **1966**, *5*, 385–415. [CrossRef]
56. Higashibayashi, S.; Onogi, S.; Srivastava, H.K.; Sastry, G.N.; Wu, Y.-T.; Sakurai, H. Stereoelectronic effect of curved aromatic structures: Favoring the unexpected endo conformation of benzylic-substituted sumanene. *Angew. Chem. Int. Ed.* **2013**, *52*, 7314–7316. [CrossRef] [PubMed]
57. Eisenberg, D.; Filatov, A.S.; Jackson, E.A.; Rabinovitz, M.; Petrukhina, M.A.; Scott, L.T.; Shenhar, R. Bicorannulenyl: Stereochemistry of a c40h18 biaryl composed of two chiral bowls. *J. Org. Chem.* **2008**, *73*, 6073–6078. [CrossRef] [PubMed]
58. Imamura, K.; Takimiya, K.; Otsubo, T.; Aso, Y. Triphenyleno[1,12-bcd:4,5-b[prime or minute]c[prime or minute]d[prime or minute]:8,9-b[double prime]c[double prime]d[double prime]]trithiophene: The first bowl-shaped heteroaromatic. *Chem. Commun.* **1999**, 1859–1860. [CrossRef]
59. Furukawa, S.; Kobayashi, J.; Kawashima, T. Development of a sila-friedel-crafts reaction and its application to the synthesis of dibenzosilole derivatives. *J. Am. Chem. Soc.* **2009**, *131*, 14192–14193. [CrossRef] [PubMed]
60. Furukawa, S.; Kobayashi, J.; Kawashima, T. Application of the sila-friedel-crafts reaction to the synthesis of [small pi]-extended silole derivatives and their properties. *Dalton Trans.* **2010**, *39*, 9329–9336. [CrossRef] [PubMed]
61. Saito, M.; Tanikawa, T.; Tajima, T.; Guo, J.D.; Nagase, S. Synthesis and structures of heterasumanenes having different heteroatom functionalities. *Tetrahedron Lett.* **2010**, *51*, 672–675. [CrossRef]
62. Tanikawa, T.; Saito, M.; Guo, J.D.; Nagase, S. Synthesis, structures and optical properties of trisilasumanene and its related compounds. *Org. Biomol. Chem.* **2011**, *9*, 1731–1735. [CrossRef] [PubMed]
63. Tanikawa, T.; Saito, M.; Guo, J.D.; Nagase, S.; Minoura, M. Synthesis, structures, and optical properties of heterasumanenes containing group 14 elements and their related compounds. *Eur. J. Org. Chem.* **2012**, *2012*, 7135–7142. [CrossRef]
64. Li, X.; Zhu, Y.; Shao, J.; Wang, B.; Zhang, S.; Shao, Y.; Jin, X.; Yao, X.; Fang, R.; Shao, X. Non-pyrolytic, large-scale synthesis of trichalcogenasumanene: A two-step approach. *Angew. Chem. Int. Ed.* **2014**, *53*, 535–538. [CrossRef] [PubMed]
65. Wang, S.; Li, X.; Hou, X.; Sun, Y.; Shao, X. Tritellurasumanene: Ultrasound assisted one-pot synthesis and extended valence adducts with bromine. *Chem. Commun.* **2016**, *52*, 14486–14489. [CrossRef] [PubMed]
66. Hou, X.; Zhu, Y.; Qin, Y.; Chen, L.; Li, X.; Zhang, H.-L.; Xu, W.; Zhu, D.; Shao, X. Tris(s,s-dioxide)-trithiasumanene: Strong fluorescence and cocrystal with 1,2,6,7,10,11-hexabutoxytriphenylene. *Chem. Commun.* **2017**, *53*, 1546–1549. [CrossRef] [PubMed]
67. Furukawa, S.; Suda, Y.; Kobayashi, J.; Kawashima, T.; Tada, T.; Fujii, S.; Kiguchi, M.; Saito, M. Triphosphasumanene trisulfide: High out-of-plane anisotropy and janus-type π-surfaces. *J. Am. Chem. Soc.* **2017**, *139*, 5787–5792. [CrossRef] [PubMed]
68. Barth, W.E.; Lawton, R.G. Dibenzo[ghi,mno]fluoranthene. *J. Am. Chem. Soc.* **1966**, *88*, 380–381. [CrossRef]
69. Scott, L.T.; Hashemi, M.M.; Meyer, D.T.; Warren, H.B. Corannulene. A convenient new synthesis. *J. Am. Chem. Soc.* **1991**, *113*, 7082–7084. [CrossRef]
70. Borchardt, A.; Fuchicello, A.; Kilway, K.V.; Baldridge, K.K.; Siegel, J.S. Synthesis and dynamics of the corannulene nucleus. *J. Am. Chem. Soc.* **1992**, *114*, 1921–1923. [CrossRef]
71. Abdourazak, A.H.; Marcinow, Z.; Sygula, A.; Sygula, R.; Rabideau, P.W. Buckybowls 2. Toward the total synthesis of buckminsterfullerene (C60): Benz[5,6]-as-indaceno[3,2,1,8,7-mnopqr]indeno[4,3,2,1-cdef] chrysene. *J. Am. Chem. Soc.* **1995**, *117*, 6410–6411. [CrossRef]
72. Mehta, G.; Shahk, S.R.; Ravikumarc, K. Towards the design of tricyclopenta [def, jkl, pqr] triphenylene ('sumanene'): A 'bowl-shaped' hydrocarbon featuring a structural motif present in C60(buckminsterfullerene). *J. Chem. Soc. Chem. Commun.* **1993**, 1006–1008. [CrossRef]
73. Seiders, T.J.; Baldridge, K.K.; Siegel, J.S. Synthesis and characterization of the first corannulene cyclophane. *J. Am. Chem. Soc.* **1996**, *118*, 2754–2755. [CrossRef]

74. Sakurai, H.; Daiko, T.; Hirao, T. A synthesis of sumanene, a fullerene fragment. *Science* **2003**, *301*, 1878. [CrossRef] [PubMed]
75. Higashibayashi, S.; Sakurai, H. Synthesis of an enantiopure syn-benzocyclotrimer through regio-selective cyclotrimerization of a halonorbornene derivative under palladium nanocluster conditions. *Chem. Lett.* **2007**, *36*, 18–19. [CrossRef]
76. Reza, A.F.G.M.; Higashibayashi, S.; Sakurai, H. Preparation of C3-symmetric homochiral syn-trisnorbornabenzenes through regioselective cyclotrimerization of enantiopure iodonorbornenes. *Chem. Asian J.* **2009**, *4*, 1329–1337. [CrossRef] [PubMed]
77. Priyakumar, U.D.; Sastry, G.N. Heterobuckybowls: A theoretical study on the structure, bowl-to-bowl inversion barrier, bond length alternation, structure-inversion barrier relationship, stability, and synthetic feasibility. *J. Org. Chem.* **2001**, *66*, 6523–6530. [CrossRef] [PubMed]
78. Hagen, S.; Bratcher, M.S.; Erickson, M.S.; Zimmermann, G.; Scott, L.T. Novel syntheses of three C30H12 bowl-shaped polycyclic aromatic hydrocarbons. *Angew. Chem. Int. Ed.* **1997**, *36*, 406–408. [CrossRef]
79. Amaya, T.; Nakata, T.; Hirao, T. Synthesis of highly strained π-bowls from sumanene. *J. Am. Chem. Soc.* **2009**, *131*, 10810–10811. [CrossRef] [PubMed]
80. Tsefrikas, V.M.; Arns, S.; Merner, P.M.; Warford, C.C.; Merner, B.L.; Scott, L.T.; Bodwell, G.J. Benzo[a]acecorannulene: Surprising formation of a new bowl-shaped aromatic hydrocarbon from an attempted synthesis of 1,2-diazadibenzo[d,m]corannulene. *Org. Lett.* **2006**, *8*, 5195–5198. [CrossRef] [PubMed]
81. Wu, Y.-T.; Hayama, T.; Baldridge, K.K.; Linden, A.; Siegel, J.S. Synthesis of fluoranthenes and indenocorannulenes: Elucidation of chiral stereoisomers on the basis of static molecular bowls. *J. Am. Chem. Soc.* **2006**, *128*, 6870–6884. [CrossRef] [PubMed]
82. Rickhaus, M.; Mayor, M.; Juricek, M. Chirality in curved polyaromatic systems. *Chem. Soc. Rev.* **2017**, *46*, 1643–1660. [CrossRef] [PubMed]
83. Suárez, M.; Branda, N.; Lehn, J.-M.; Decian, A.; Fischer, J. Supramolecular chirality: Chiral hydrogen-bonded supermolecules from achiral molecular components. *Helv. Chim. Acta* **1998**, *81*, 1–13. [CrossRef]
84. Dalla Cort, A.; Mandolini, L.; Pasquini, C.; Schiaffino, L. "Inherent chirality" and curvature. *New J. Chem.* **2004**, *28*, 1198–1199. [CrossRef]
85. Szumna, A. Inherently chiral concave molecules-from synthesis to applications. *Chem. Soc. Rev.* **2010**, *39*, 4274–4285. [CrossRef] [PubMed]
86. Supramolecular chirality. In *Topics in Current Chemistry*; Crego-Calama, M.; Reinhoudt, D.N., Eds.; Springer: Berlin/Heidelberg, Germany, 2006; Volume 265, p. 312.
87. Yao, J.; Wu, W.; Liang, W.; Feng, Y.; Zhou, D.; Chruma, J.J.; Fukuhara, G.; Mori, T.; Inoue, Y.; Yang, C. Temperature-driven planar chirality switching of a pillar[5]arene-based molecular universal joint. *Angew. Chem. Int. Ed.* **2017**, *56*, 6869–6873. [CrossRef] [PubMed]
88. Kaewmati, P.; Tan, Q.; Higashibayashi, S.; Yakiyama, Y.; Sakurai, H. Synthesis of triaryltriazasumanenes. *Chem. Lett.* **2017**, *46*, 146–148. [CrossRef]
89. Huang, Q.; Jiang, L.; Liang, W.; Gui, J.; Xu, D.; Wu, W.; Nakai, Y.; Nishijima, M.; Fukuhara, G.; Mori, T.; et al. Inherently chiral azonia[6]helicene-modified β-cyclodextrin: Synthesis, characterization, and chirality sensing of underivatized amino acids in water. *J. Org. Chem.* **2016**, *81*, 3430–3434. [CrossRef] [PubMed]
90. Yan, Z.; Huang, Q.; Liang, W.; Yu, X.; Zhou, D.; Wu, W.; Chruma, J.J.; Yang, C. Enantiodifferentiation in the photoisomerization of (z,z)-1,3-cyclooctadiene in the cavity of γ-cyclodextrin–curcubit[6]uril-wheeled [4]rotaxanes with an encapsulated photosensitizer. *Org. Lett.* **2017**, *19*, 898–901. [CrossRef] [PubMed]
91. Gui, J.-C.; Yan, Z.-Q.; Peng, Y.; Yi, J.-G.; Zhou, D.-Y.; Su, D.; Zhong, Z.-H.; Gao, G.-W.; Wu, W.-H.; Yang, C. Enhanced head-to-head photodimers in the photocyclodimerization of anthracenecarboxylic acid with a cationic pillar [6] arene. *Chin. Chem. Lett.* **2016**, *27*, 1017–1021. [CrossRef]
92. Yao, J.; Yan, Z.; Ji, J.; Wu, W.; Yang, C.; Nishijima, M.; Fukuhara, G.; Mori, T.; Inoue, Y. Ammonia-driven chirality inversion and enhancement in enantiodifferentiating photocyclodimerization of 2-anthracenecarboxylate mediated by diguanidino-γ-cyclodextrin. *J. Am. Chem. Soc.* **2014**, *136*, 6916–6919. [CrossRef] [PubMed]
93. Liang, W.; Yang, C.; Nishijima, M.; Fukuhara, G.; Mori, T.; Mele, A.; Castiglione, F.; Caldera, F.; Trotta, F.; Inoue, Y. Cyclodextrin nanosponge-sensitized enantiodifferentiating photoisomerization of cyclooctene and 1,3-cyclooctadiene. *Beilstein J. Org. Chem.* **2012**, *8*, 1305–1311. [CrossRef] [PubMed]

94. Wang, Q.; Yang, C.; Ke, C.; Fukuhara, G.; Mori, T.; Liu, Y.; Inoue, Y. Wavelength-controlled supramolecular photocyclodimerization of anthracenecarboxylate mediated by γ-cyclodextrins. *Chem. Commun.* **2011**, *47*, 6849–6851. [CrossRef] [PubMed]
95. Fujikawa, T.; Preda, D.V.; Segawa, Y.; Itami, K.; Scott, L.T. Corannulene–helicene hybrids: Chiral π-systems comprising both bowl and helical motifs. *Org. Lett.* **2016**, *18*, 3992–3995. [CrossRef] [PubMed]
96. Yanney, M.; Fronczek, F.R.; Sygula, A. Corannulene subunit acts as a diene in a cycloaddition reaction: Synthesis of C80H32 corannulyne tetramer. *Org. Lett.* **2012**, *14*, 4942–4945. [CrossRef] [PubMed]
97. Yanney, M.; Fronczek, F.R.; Henry, W.P.; Beard, D.J.; Sygula, A. Cyclotrimerization of corannulyne: Steric hindrance tunes the inversion barriers of corannulene bowls. *Eur. J. Org. Chem.* **2011**, *2011*, 6636–6639. [CrossRef]
98. Kawasumi, K.; Zhang, Q.; Segawa, Y.; Scott, L.T.; Itami, K. A grossly warped nanographene and the consequences of multiple odd-membered-ring defects. *Nat. Chem.* **2013**, *5*, 739–744. [CrossRef] [PubMed]
99. Amaya, T.; Mori, K.; Wu, H.-L.; Ishida, S.; Nakamura, J.-I.; Murata, K.; Hirao, T. Synthesis and characterization of [small pi]-extended bowl-shaped [small pi]-conjugated molecules. *Chem. Commun.* **2007**, 1902–1904. [CrossRef]
100. Chen, R.; Lu, R.-Q.; Shi, P.-C.; Cao, X.-Y. Corannulene derivatives for organic electronics: From molecular engineering to applications. *Chin. Chem. Lett.* **2016**, *27*, 1175–1183. [CrossRef]
101. Kobayashi, S.-i.; Mori, S.; Iida, S.; Ando, H.; Takenobu, T.; Taguchi, Y.; Fujiwara, A.; Taninaka, A.; Shinohara, H.; Iwasa, Y. Conductivity and field effect transistor of la2@C80 metallofullerene. *J. Am. Chem. Soc.* **2003**, *125*, 8116–8117. [CrossRef] [PubMed]
102. Kato, H.; Kanazawa, Y.; Okumura, M.; Taninaka, A.; Yokawa, T.; Shinohara, H. Lanthanoid endohedral metallofullerenols for MRI contrast agents. *J. Am. Chem. Soc.* **2003**, *125*, 4391–4397. [CrossRef] [PubMed]
103. Petrukhina, M.A.; Scott, L.T. Coordination chemistry of buckybowls: From corannulene to a hemifullerene. *Dalton Trans.* **2005**, 2969–2975. [CrossRef] [PubMed]
104. Vecchi, P.A.; Alvarez, C.M.; Ellern, A.; Angelici, R.J.; Sygula, A.; Sygula, R.; Rabideau, P.W. Flattening of a curved-surface buckybowl (corannulene) by η6 coordination to {cp*ru}+. *Organometallics* **2005**, *24*, 4543–4552. [CrossRef]
105. Zhu, B.; Ellern, A.; Sygula, A.; Sygula, R.; Angelici, R.J. η6-Coordination of the curved carbon surface of corannulene (C20H10) to (η6-arene)M^{2+} (M = Ru, Os). *Organometallics* **2007**, *26*, 1721–1728. [CrossRef]
106. Zabula, A.V.; Spisak, S.N.; Filatov, A.S.; Rogachev, A.Y.; Clerac, R.; Petrukhina, M.A. Supramolecular trap for a transient corannulene trianion. *Chem. Sci.* **2016**, *7*, 1954–1961. [CrossRef]
107. Kameno, Y.; Ikeda, A.; Nakao, Y.; Sato, H.; Sakaki, S. Theoretical study of M(PH3)2 complexes of C60, corannulene (C20H10), and sumanene (C21H12) (M = Pd or Pt). Unexpectedly large binding energy of M(PH3)2(C60). *J. Phys. Chem. A* **2005**, *109*, 8055–8063. [CrossRef] [PubMed]
108. Agnes, M.; Nitti, A.; Vander Griend, D.A.; Dondi, D.; Merli, D.; Pasini, D. A chiroptical molecular sensor for ferrocene. *Chem. Commun.* **2016**, *52*, 11492–11495. [CrossRef] [PubMed]
109. Caricato, M.; Leza, N.J.; Roy, K.; Dondi, D.; Gattuso, G.; Shimizu, L.S.; Vander Griend, D.A.; Pasini, D. A chiroptical probe for sensing metal ions in water. *Eur. J. Org. Chem.* **2013**, *2013*, 6078–6083. [CrossRef]
110. Caricato, M.; Coluccini, C.; Dondi, D.; Vander Griend, D.A.; Pasini, D. Nesting complexation of C60 with large, rigid d2 symmetrical macrocycles. *Org. Biomol. Chem.* **2010**, *8*, 3272–3280. [CrossRef] [PubMed]
111. Caricato, M.; Sharma, A.K.; Coluccini, C.; Pasini, D. Nanostructuring with chirality: Binaphthyl-based synthons for the production of functional oriented nanomaterials. *Nanoscale* **2014**, *6*, 7165–7174. [CrossRef] [PubMed]
112. Nitti, A.; Pacini, A.; Pasini, D. Chiral nanotubes. *Nanomaterials* **2017**, *7*, 167. [CrossRef] [PubMed]
113. Bancu, M.; Rai, A.K.; Cheng, P.; Gilardi, R.D.; Scott, L.T. Corannulene polysulfides: Molecular bowls with multiple arms and flaps. *Synlett* **2004**, *2004*, 173–176.
114. Xiao, W.; Ernst, K.-H.; Palotas, K.; Zhang, Y.; Bruyer, E.; Peng, L.; Greber, T.; Hofer, W.A.; Scott, L.T.; Fasel, R. Microscopic origin of chiral shape induction in achiral crystals. *Nat. Chem.* **2016**, *8*, 326–330. [CrossRef] [PubMed]
115. Schunack, M.; Lægsgaard, E.; Stensgaard, I.; Johannsen, I.; Besenbacher, F. A chiral metal surface. *Angew. Chem. Int. Ed.* **2001**, *40*, 2623–2626. [CrossRef]
116. Karageorgaki, C.; Ernst, K.-H. A metal surface with chiral memory. *Chem. Commun.* **2014**, *50*, 1814–1816. [CrossRef] [PubMed]